Weakly Coordinating Al-, Nb-, Ta-, Y-, and La-Based Perfluoroaryloxymetalate Anions as Cocatalyst Components for Single-Site Olefin Polymerization

Matthew V. Metz, Yimin Sun,† Charlotte L. Stern, and Tobin J. Marks*

Department of Chemistry, Northwestern University, 2145 Sheridan Road, Evanston, Illinois 60208-3113

Received February 5, 2002

Reaction of $LiAlH_4$ with 4.0 equiv of HOC_6F_5 in toluene leads to H_2 evolution and formation of $Li^+Al(OC_6F_5)_4^-$; subsequent metathesis with Ph_3CCl then yields the corresponding trityl tetrakis(pentafluorophenoxo)aluminate, $Ph_3C^+Al(OC_6F_5)_4^-$ (**4**). The pentachlorides MCl_5 (M = Nb, Ta) undergo reaction with 6.0 equiv of $LiOC_6F_5$ in Et_2O to afford crystalline $Li(OEt_2)_n^+$-{$[M(OC_6F_5)_4(\mu_2\text{-}OC_6F_5)_2]_2Li$}·$C_7H_8$ salts (M = Nb, n = 4 (**5a**); M = Ta, n = 3 (**5b**)), which can be cleanly converted with Ph_3CCl to the corresponding mononuclear, thermally stable $Ph_3C^+M(OC_6F_5)_6^-$ salts (M = Nb (**6a**); M = Ta (**6b**)) in high yield. X-ray diffraction analysis of **6** reveals six-coordinate metal centers with substantial distortion of the M−O−C_6F_5 linkages from linearity. The reactivity and cocatalytic characteristics of **6** were investigated with respect to a series of metallocene dimethyls. For sterically unencumbered metallocenes, facile $C_6F_5O^-$ transfer from Nb/Ta to Zr/Ti is observed. However, $(C_5Me_5)_2ZrMe(THF\text{-}d_8)^+$-$Nb(OC_6F_5)_6^-$ (**7**) is formed in the reaction of **6a** with $(C_5Me_5)_2ZrMe_2$ in THF-d_8. In situ activation of $(C_5Me_5)_2ZrMe_2$ and $(C_5Me_4H)_2ZrMe_2$ with **4** and **6** yields efficient ethylene polymerization catalysts, having activities comparable to those of $Ph_3C^+B(C_6F_5)_4^-$-activated systems under identical polymerization conditions. To impede aryloxide ring transfer, a bulkier ligand, 2-nonafluorobiphenoxide ($C_{12}F_9O^-$), was combined with highly oxophilic Y^{3+} and La^{3+} centers. Reaction of $M[CH(SiMe_3)_2]_3$ (M = Y, La) with 4.0 equiv of 2-$HOC_{12}F_9$ results in the clean formation of $M(OC_{12}F_9)_3(HOC_{12}F_9)$ complexes (M = Y (**9a**); M = La, (**9b**)) in high yield. When **9** is paired with metallocene dimethyl precursors, even sterically open precatalysts such as $CGCTiMe_2$ (CGC = $Me_2Si(C_5Me_4)^tBuN$) or $(C_5H_5)_2ZrMe_2$ yield highly active ethylene polymerization systems.

Introduction

In single-site α-olefin polymerization catalysis, a precatalyst (usually a group 4-based metallocene or similar complex)[1,2] and a cocatalyst,[3] typically group 13-based and containing metal/metalloid−carbon bonds, e.g., methylalumoxane (MAO),[4] $MAr^F_xAr_{3-x}$,[5] $MAr^F_4{}^-$ [6] (M = B, Al; Ar^F = fluoroaryl group), etc., are combined to form the active catalytic species consisting of a cationic metal center and a weakly coordinating anion (**1**). Due to their structurally well-defined chemical

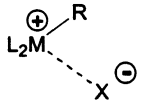

1

nature and high cocatalytic activity, the perfluoroarylboranes, -borates, and -aluminates are of consider-

† Current address: Uniroyal Chemical Company, 280 Elm St., Building 310, Naugatuck, CT 06770.

(1) For recent reviews see: (a) Chum, P. S.; Kruper, W. J.; Guest, M. J. *Adv. Mater.* **2000**, *12*, 1759−1767. (b) Gladysz, J. A., Ed. *Chem. Rev.* **2000**, *100* (special issue on "Frontiers in Metal-Catalyzed Polymerization"). (c) Marks, T. J., Stevens, J. C., Eds. *Top. Catal.* **1999**, *7*, 1 (special volume on "Advances in Polymerization Catalysis. Catalysts and Processes"). (d) Scheirs J.; Kaminsky, W. *Metallocene-Based Polyolefins: Preparation, Properties, and Technology*; John Wiley & Sons: New York, 1999; Vols. 1 and 2. (e) Kaminsky, W. *Metalorganic Catalysts for Synthesis and Polymerization: Recent Results by Ziegler−Natta and Metallocene Investigations*; Springer-Verlag: Berlin, 1999. (f) Jordan, R. F. *J. Mol. Catal.* **1998**, *128*, 1 (special issue on metallocene and single-site olefin catalysts). (g) McKnight, A. L.; Waymouth, R. M. *Chem. Rev.* **1998**, *98*, 2587−2598 (constrained geometry polymerization catalysts). (h) Piers, W. E. *Chem. Eur. J.* **1998**, *4*, 13−18. (i) Kaminsky, W.; Arndt, M. *Adv. Polym. Sci.* **1997**, *127*, 143−187. (j) Bochmann, M. *J. Chem. Soc., Dalton Trans.* **1996**, 255−270. (k) Brintzinger, H. H.; Fischer, D.; Mülhaupt, R.; Rieger, B.; Waymouth, R. M. *Angew. Chem., Int. Ed. Engl.* **1995**, *34*, 1143−1170. (l) Marks, T. J. *Acc. Chem. Res.* **1992**, *25*, 57−65.

(2) For nonmetallocene references see: (a) Matsui, S.; Fujita, T. *Catal. Today* **2001**, *66*, 63−73. (b) Younkin, T. R.; Connor, E. F.; Henderson, J. I.; Friedrich, S. K.; Grubbs, R. H.; Bansleben, D. A. *Science* **2000**, *287*, 460−462. (c) Ittel, S. D.; Johnson, L. K.; Brookhart, M. *Chem. Rev.* **2000**, *100*, 1169−1203. (d) Britovsek, G. J. P.; Gibson, V. C.; Wass, D. F. *Angew. Chem., Int. Ed.* **1999**, *38*, 428−447.

(3) For recent reviews of cocatalysts and weakly coordinating anions see: (a) Pedeutour, J.-N.; Radhakrishnan, K.; Cramail, H.; Deffieux, A. *Macromol. Rapid Commun.* **2001**, *22*, 1095−1123. (b) Chen, Y-. X.; Marks, T. J. *Chem. Rev.* **2000**, *100*, 1391−1434. (c) Piers, W. E. *Chem. Eur. J.* **1998**, *4*, 13−18. (d) Reed, C. A. *Acc. Chem. Res.* **1998**, *31*, 133−139. (e) Piers, W. E.; Chivers, T. *Chem. Soc. Rev.* **1997**, *26*, 345−354. (f) Strauss, S. H. *Chem. Rev.* **1993**, *93*, 927−942.

(4) (a) Barron, A. R. In *Metallocene-Based Polyolefins*; Scheirs, J., Kaminsky, W., Eds.; John Wiley & Sons Ltd.: Chichester, UK, 2000; pp 33−67. (b) Coevoet, D.; Cramail, H.; Deffieux, A. *Macromol. Chem. Phys.* **1998**, *199*, 1459−1464. (c) Reddy, S. S.; Sivaram, S. *Prog. Polym. Sci.* **1995**, *20*, 309−367. (d) Harlan, C. J.; Bott, S. G.; Barron, A. R. *J. Am. Chem. Soc.* **1995**, *117*, 6465−6474. (e) Sishta, C.; Hathorn, R. M.; Marks, T. J. *J. Am. Chem. Soc.* **1992**, *114*, 1112−1114. (f) Pasynkiewicz, S. *Polyhedron* **1990**, *9*, 429−53.

10.1021/om020087s CCC: $22.00
Publication on Web 08/09/2002

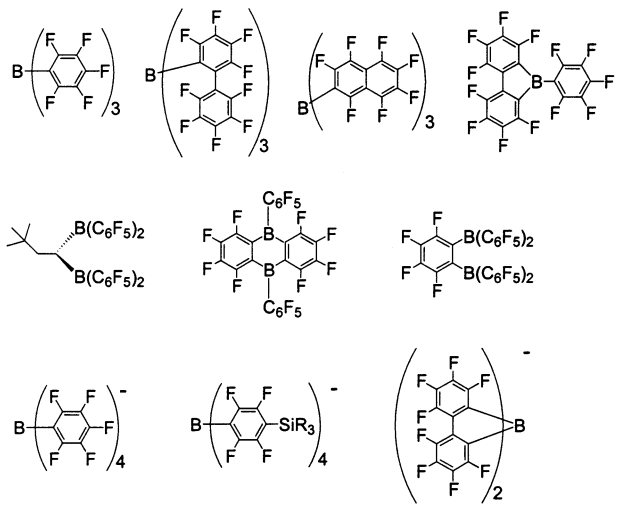

Figure 1. Representative perfluoroaryl borane and borate cocatalyst structures used in single-site olefin polymerization.

able current scientific and technological interest (Figure 1). Experimental results to date, supported by theoretical analyses,[7] argue that many of the properties of such catalyst systems are intimately connected with the nature of the cation−anion interaction in ways that are presently not well-understood. The size, shape, charge, electronic structure, and potential ligational characteristics of the anion can have profound effects on catalyst activity, thermal stability, chain transfer characteristics, stereoselection, etc.[4−6,8] Nevertheless, the number of available cocatalyst families is currently rather limited and has so far impeded a broad, systematic study of cation−anion effects.

To truly broaden the available cocatalytic options for single-site Ziegler−Natta olefin polymerization systems, it is intriguing to inquire whether viable cocatalyst anions devoid of group 13 elements and element−carbon bonds can be synthesized and whether they form stable catalytic species when paired with group 4 hydrocarbyls. Recent results[5i,j] suggest that by increasing the steric bulk of the cocatalyst anion, hence decreasing the strength of localized ion pairing, catalyst systems with much higher polymerization activities can be achieved. To develop new, more sterically encumbered cocatalysts, a linker was sought to introduce between the metal/metalloid anionic center and an inert perfluoroaryl periphery. Oxygen was chosen as the linker because it forms very strong bonds to the early transition metal and rare earth ions, which were in turn chosen as the non-group 13 cores of the new cocatalyst structures. Although oxygen and alcohols are known poisons for homogeneous Ziegler−Natta polymerization systems, it was hypothesized that by screening the oxygen atoms with sterically encumbered perfluoroaryl substituents and by decreasing the nucleophilicity of the oxygen atoms with strongly electron-withdrawing perfluoroaryl rings, stable cocatalyst anions could be formed. The following contribution describes the synthesis, characterization, and cocatalytic features of a new series of sterically encumbered metalloid, transition metal, and rare earth cocatalysts/counteranions based on pentafluorophenoxide (**2**; $C_6F_5O^-$) and nonafluorobiphenoxide (**3**; $C_{12}F_9O^-$) substituents.[9]

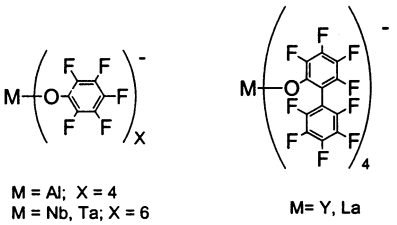

The first class of perfluoroaryloxide cocatalyst anions investigated was based on Al^{III}, Nb^{V}, and Ta^{V} centers and the $C_6F_5O^-$ ligand. It will be seen that the trityl salts $[Ph_3C]^+[Al(OC_6F_5)_4]^-$ (**4**), $[Ph_3C]^+[Nb(OC_6F_5)_6]^-$ (**6a**), and $[Ph_3C]^+[Ta(OC_6F_5)_6]^-$ (**6b**) form active ethylene polymerization systems, but only when paired with sterically demanding metallocenium cations. Facile $C_6F_5O^-$ transfer to the cationic metallocene occurs when less encumbered metallocenes, such as $(C_5H_5)_2ZrMe_2$,

(5) (a) Chen, E. Y.-X.; Kruper, W. J.; Roof, G. R.; Wilson, D. R. *J. Am. Chem. Soc.* **2001**, *123*, 745−746. (b) Zhou, J.; Lancaster, S. J.; Walker, D. A.; Beck, S.; Thornton-Pett, M.; Bochmann, M. *J. Am. Chem. Soc.* **2001**, *123*, 223−237. (c) Metz, M. V.; Schwartz, D. J.; Stern, C. L.; Nickias, P. N.; Marks, T. J. *Angew. Chem., Int. Ed.* **2000**, *39*, 1312−1316. (d) Chase, P. A.; Piers, W. E.; Patrick, B. O. *J. Am. Chem. Soc.* **2000**, *122*, 12911−12912. (e) Klosin, J.; Roof, G. R.; Chen, E. Y.-X.; Abboud, K. A. *Organometallics* **2000**, *19*, 4684−4686. (f) LaPointe, R. E.; Roof, G. R.; Abboud, K. A.; Klosin, J. *J. Am. Chem. Soc.* **2000**, *122*, 9560−9561. (g) Williams, V. C.; Irvine, G. J.; Piers, W. E.; Li, Z.; Collins, S.; Clegg, W.; Elsegood, M. R. J.; Marder, T. B. *Organometallics* **2000**, *19*, 1619−1621. (h) Williams, V. C.; Piers, W. E.; Clegg, W.; Elsegood, M. R. J.; Collins, S.; Marder, T. B. *J. Am. Chem. Soc.* **1999**, *121*, 3244−3245. (i) Luo, L.; Marks, T. J. *Top. Catal.* **1999**, *7*, 97−106. (j) Kohler, K.; Piers, W. E. *Can. J. Chem.* **1998**, *76*, 1249−1255. (k) Li, L.; Marks, T. J. *Organometallics* **1998**, *17*, 3996−4003. (l) Chen, Y.-X.; Metz, M. V.; Li, L.; Stern, C. L.; Marks, T. J. *J. Am. Chem. Soc.* **1998**, *120*, 6287−6305. (m) Deck, P. A.; Beswick, C. L.; Marks, T. J. *J. Am. Chem. Soc.* **1998**, *120*, 1772−1784. (n) Temme, B.; Erker, G.; Karl, J.; Luftmann, H.; Frohlich, R.; Kotila, S. *Angew. Chem., Int. Ed. Engl.* **1995**, *34*, 1755−1757. (o) Yang, X.; Stern, C. L.; Marks, T. J. *J. Am. Chem. Soc.* **1994**, *116*, 10015−10031. (p) Jia, L.; Yang, X.; Stern, C. L.; Marks, T. J. *Organometallics* **1994**, *13*, 3755−3757.

(6) (a) Jia, L.; Yang, X.; Stern, C. L.; Marks, T. J. *Organometallics* **1997**, *16*, 842−857. (b) Chien, J. C. W.; Tsai, W. M.; Rausch, M. D. *J. Am. Chem. Soc.* **1991**, *113*, 8570−8571. (c) Yang, X.; Stern, C.; Marks, T. J. *Organometallics* **1991**, *10*, 840−842. (d) Ewen, J. A.; Elder, M. J. (Fina Technology, Inc.) *Preparation of Metallocene Catalysts for Polymerization of Olefins*; EP0426637, May 8, 1991. (e) Hlatky, G. G.; Upton, D. J.; Turner, H. W. (Exxon Chemical Patents, Inc.) *Supported Ionic Metallocene Catalysts for Olefin Polymerization*; WO 9109882, July 7, 1991. (f) Turner, H. W. (Exxon Chemical Patents, Inc.) *Soluble Catalysts for Polymerization of Olefins*; EP 277004A1, Aug 3, 1988.

(7) (a) Lanza, G.; Fragalà, I. L.; Marks, T. J. *Organometallics* **2001**, *20*, 4006−4017. (b) Vanka, K.; Ziegler, T. *Organometallics* **2001**, *20*, 905−913. (c) Lanza, G.; Fragalà, I. L.; Marks, T. J. *J. Am. Chem. Soc.* **2000**, *122*, 12764−12777. (d) Chan, M. S. W.; Ziegler, T. *Organometallics* **2000**, *19*, 5182−5189. (e) Rappé, A. K.; Skiff, W. M.; Casewit, C. J. *Chem. Rev.* **2000**, *100*, 1435−1456. (f) Vanka, K.; Chan, M. S. W.; Pye, C.; Ziegler, T. *Organometallics* **2000**, *19*, 1841−1849. (g) Chan, M. S. W.; Vanka, K.; Pye, C. C.; Ziegler, T. *Organometallics* **1999**, *18*, 4624−4636. (h) Lanza, G.; Fragalà, I. L. *Top. Catal.* **1999**, *15*, 45−60. (i) Lanza, G.; Fragalà, I. L.; Marks, T. J. *J. Am. Chem. Soc.* **1998**, *120*, 8257−8258. (j) Fusco, R.; Longo, L.; Proto, A.; Masi; F.; Garbasi, F. *Macromol. Rapid Commun.* **1998**, *19*, 257−262. (k) Fusco, R.; Longo, L.; Masi, F.; Garbasi, F. *Macromolecules* **1997**, *30*, 7673−7685. (l) Fusco, R.; Longo, L.; Masi, F.; Garbasi, F. *Macromol. Rapid Commun.* **1997**, *18*, 433−441.

(8) (a) Shiomura, T.; Uchikawa, N.; Asanuma, T.; Sugimoto, R.; Fujio, I.; Kimura, S.; Harima, S.; Akiyama, M.; Kohno, M.; Inoue, N. In *Metallocene-Based Polyolefins*; Scheirs, J., Kaminsky, W., Eds.; John Wiley & Sons Ltd.: Chichester, UK, 2000; Vol. 1, pp 437−465. (b) Rhodes, B.; Chien, J. C. W.; Rausch, M. D. *Organometallics* **1998**, *17*, 1931−1933. (c) Shiomura, T.; Asanuma, T.; Inoue, N. *Macromol. Rapid Commun.* **1996**, *17*, 9−14. (d) Giardello, M. A.; Eisen, M. S.; Stern, C. L.; Marks, T. J. *J. Am. Chem. Soc.* **1995**, *117*, 12114−12129. (e) Siedle, A. R.; Hanggi, B.; Newmark, R. A.; Mann, K. R.; Wilson, T. *Macromol. Symp.* **1995**, *89*, 299−305. (f) Eisch, J. J.; Pombrik, S. I.; Gurtzgen, S.; Rieger, R.; Uzick, W. *Stud. Surf. Sci. Catal.* **1994**, *89*, 221−235.

(9) Portions of this work previously communicated: Sun, Y.; Metz, M. V.; Stern, C. L.; Marks, T. J. *Organometallics* **2000**, *19*, 1625−1627.

are employed as organo-group 4 catalysts. To expand the scope of perfluorophenoxide cocatalysts and to improve their catalytic versatility, it was necessary to reduce phenoxide group transfer to the metallocene. This was accomplished in two ways. To increase the steric bulk of the cocatalyst anions, pentafluorophenoxide ligands were replaced with more sterically encumbered nonafluorobiphenoxide ligands. To decrease the propensity for perfluoroaryloxide ring transfer to the metallocenium components, trivalent lanthanides were chosen as the central core because of their high oxophilicity. Thus, cocatalysts $Y(OC_{12}F_9)_3(HOC_{12}F_9)$ (**9a**) and $La(OC_{12}F_9)_3(HOC_{12}F_9)$ (**9b**) were synthesized and studied as homogeneous single-site polymerization cocatalysts. The present results demonstrate that effective cocatalysts need not contain metalloid/metal−carbon bonds and that the properties of the resulting metallocenium cation−anion pairs are sensitive to both the counteranion core structure as well as to the metallocene ancillary ligation.[9]

Experimental Section

Materials and Methods. All manipulations of air-sensitive materials were carried out with rigorous exclusion of oxygen and moisture in flame-dried Schlenk-type glassware on a dual-manifold Schlenk line interfaced to a high-vacuum line (10^{-6} Torr) or in a nitrogen-filled Vacuum Atmospheres glovebox with a high capacity recirculator (<1 ppm of O_2). Argon (Matheson, prepurified), ethylene (Matheson, polymerization grade), and propylene (Matheson, polymerization grade) were purified by passage through a Matheson Gas Products OXISORB-W column or by passage through a supported MnO oxygen-removal column and an activated Davison 4 Å molecular sieve column. All solvents were distilled before use under dry nitrogen over appropriate drying agents (Et_2O, THF, from sodium benzophenone ketyl; pentane, hexane, toluene from Na/K alloy or by passage though solvent purification columns;[10] CH_2Cl_2, from CaH_2). All solvents for high-vacuum line manipulations were subsequently stored in vacuo over Na/K alloy for nonhalogenated solvents or over P_2O_5 for halogenated solvents, in Teflon-valved bulbs. Benzene-d_6, toluene-d_8, methylenechloride-d_2, and THF-d_8 (Cambridge Laboratories; all 99+ atom % D) used for NMR-scale reactions were stored in vacuo over Na/K alloy (benzene-d_6, THF-d_8) or over Davison 4 Å molecular sieves (methylenechloride-d_2) in resealable bulbs and were vacuum transferred immediately prior to use. The reagent C_6F_5Br (Aldrich) was vacuum distilled from P_2O_5 prior to use. The reagents $TiCl_4$, $ZrCl_4$, BCl_3 (gas or 1.0 M in hexanes), $LiAlH_4$, *n*-BuLi (1.6 M in hexanes), MeLi (1.0 M in diethyl ether), MCl_5 (M = Nb, Ta), C_6F_5OH, Ph_3CCl, and 50% H_2O_2 were purchased from Aldrich and used as received except that C_6F_5OH was dried over Davison 4 Å molecular sieves as a pentane solution, and Ph_3CCl was recrystallized from pentane. The organometallic reagents $Y(CH(SiMe_3)_2)_3$,[11] $La(CH(SiMe_3)_2)_3$,[12] Cp_2ZrMe_2,[13] $Me_2Si(C_5Me_4)(^tBuN)TiMe_2$,[14] (CGCTiMe$_2$), CGCZrMe$_2$,[14] $Me_2Si(Ind)_2ZrMe_2$,[15] $(C_5Me_4H)_2ZrMe_2$,[16] $(C_5Me_5)_2ZrMe_2$,[16] and $Ph_3C^+B(C_6F_5)_4^-$ [17] were prepared by published procedures.

Physical and Analytical Measurements. NMR spectra were recorded on Varian VXR 300 (FT 300 MHz, ^1H; 75 MHz, ^{13}C), Gemini-300 (FT 300 MHz, ^1H; 75 MHz, ^{13}C; 282 MHz, ^{19}F), or Mercury 400 (FT 400 MHz, ^1H; 100 MHz, ^{13}C; 376 MHz, ^{19}F) instruments. Chemical shifts for ^1H and ^{13}C spectra were referenced to internal solvent resonances and are reported relative to tetramethylsilane. ^{19}F NMR spectra were referenced to external $CFCl_3$. NMR experiments on air-sensitive samples were conducted in Teflon valve-sealed sample tubes (J. Young). Elemental analyses were performed by Midwest Microlab, Indianapolis, IN. Melting temperatures of polymers were measured by DSC (DSC 2920, TA Instruments, Inc.) from the second scan with a heating rate of 10 °C/min. GPC analyses of polymers were recorded by Dow Chemical Company on a Waters Alliance GPCV 2000 relative to polystyrene standards.

Synthesis of $Ph_3C^+Al(OC_6F_5)_4^-$ (4). A solution of $LiAlH_4$ (2.0 mL, 1.0 M, 2.0 mmol) in Et_2O was added to a Schlenk flask via syringe. At room temperature, a solution of C_6F_5OH (6.7 mL, 1.2 M, 8.4 mmol) in toluene was added to a slurry of the $LiAlH_4$ in toluene (50 mL). The mixture was heated to 85 °C and stirred overnight. After removing the solvent under vacuum, the flask was transferred to the glovebox, and solid Ph_3CCl (0.552 g, 1.98 mmol) was added to the flask. The flask was next transferred from the glovebox to the high-vacuum line. Under vacuum, pentane (35 mL) was condensed in. The mixture was allowed to warm to room temperature and then stirred for 4 h. Removing the solvent under vacuum gave dark red material. Extraction with CH_2Cl_2 (20 mL), filtration, evaporation of the solvent, and washing with pentane gave $Ph_3C^+Al(C_6F_5)_4^-$, a bright-red oily material (0.58 g), in 29% yield. ^1H NMR (CD_2Cl_2, 23 °C): δ 8.27(t, 1 H, J_{H-H} = 7.5 Hz), 7.89(tr, 2 H, J_{H-H} = 8.0 Hz), 7.66(d, 2 H, J_{H-H} = 8.2 Hz). ^{19}F NMR (CD_2Cl_2, 23 °C): δ −162.04 (d, 2 F, *o*-F, J_{F-F} = 21.4 Hz), −166.72 (tr, 2 F, *p*-F, J_{F-F} = 20.6 Hz), −173.81 (tr, br, 1 F, *m*-F). Anal. Calcd for $C_{43}H_{15}O_4F_{20}Al$: C, 51.51; H, 1.51. Found: C, 50.90; H, 1.48.

Synthesis of $Li(OEt_2)_4^+\{[Nb(OC_6F_5)_4(\mu_2\text{-}OC_6F_5)_2]_2Li\}\cdot C_7H_8$ (5a). Solid $NbCl_5$ (0.765 g, 2.83 mmol) and $LiOC_6F_5$ (3.23 g, 6 × 2.83 mmol) were added to a reaction flask in the glovebox. The flask was next transferred from the glovebox to the high-vacuum line. On the vacuum line, Et_2O (50 mL) was condensed in, and the mixture stirred overnight at room temperature. After removing the Et_2O under vacuum, toluene (50 mL) was condensed in, and the solution was heated to 50 °C and filtered. Slow cooling of the solution to −20 °C afforded yellow crystalline $[Li(OEt_2)_4]^+\{[Nb(OC_6F_5)_4(\mu_2\text{-}OC_6F_5)_2]_2Li\}^-\cdot(C_7H_8)$ (2.0 g) in 51% yield. ^1H NMR (C_6D_6, 23 °C): δ 3.04 (q, 4 H, $O(CH_2CH_3)_2$ J_{H-H} = 7.1 Hz), 0.84 (tr, 6 H, $O(CH_2CH_3)_2$ J_{H-H} = 7.1 Hz). ^{19}F NMR (C_6D_6, 23 °C): δ −161.6 (br d, 2 F, *o*-F), −163.8 (br, 3 F, *p*/*m*-F). Anal. Calcd for $C_{95}H_{48}O_{16}F_{60}Li_2Nb_2$: C, 40.97; H, 1.74; F, 40.93. Found: C, 41.36; H, 1.58; F, 40.71.

Synthesis of $Ph_3C^+Nb(OC_6F_5)_6^-$ (6a). $Li(OEt_2)_4^+\{[Nb(OC_6F_5)_4(\mu_2\text{-}OC_6F_5)_2]_2Li\}\cdot C_7H_8$ (1.91 g, 6.84 × 10^{-4} mol) and Ph_3CCl (0.389 g, 2 × 6.89 × 10^{-4} mol) were added to a reaction flask in the glovebox. The flask was next transferred from the glovebox to the high-vacuum line. On the vacuum line, pentane (50 mL) was condensed in. The mixture was then allowed to

(10) Pangborn, A. B.; Giardello, M. A.; Grubbs, R. H.; Rosen, R. K.; Timmers, F. J. *Organometallics* **1996**, *15*, 1518−1520.

(11) Barker, G. K.; Lappert, M. F. *J. Organomet. Chem.* **1974**, *76*, C45−C56.

(12) Hitchcock, P. B.; Lappert, M. F.; Smith, R. G.; Bartlett, R. A.; Power, P. P. *J. Chem. Soc., Chem. Commun.* **1988**, 1007−1009.

(13) Samuel, E.; Rausch, M. D. *J. Am. Chem. Soc.* **1973**, *95*, 6263−6267.

(14) (a) Stevens, J. C.; Timmers, F. J.; Wilson, D. R.; Schmidt, G. F.; Nickias, P. N.; Rosen, R. K.; Knight, G. W.; Lai, S. Y. (Dow Chemical Co.) *Constrained Geometry Addition Polymerization Catalysts, Processes for Their Preparation, Precursors Therefor, Methods of Use, and Novel Polymers Formed Therewith*; EP0416815, Mar 13, 1991. (b) Canich, J. M.; Hlatky, G. G.; Turner, H. W. (Exxon Chemical Patents, Inc.) *Aluminum-Free Monocyclopentadienyl Metallocene Catalysts for Olefin Polymerization*; WO-9200333 A2, Jan 9, 1992. (c) Canich, J. A. M. (Exxon Chemical Patents, Inc.) *Olefin Polymerization Catalysts*; EP-420436A1, April 3, 1991.

(15) (a) Herrmann, W. A.; Herdtweck, E.; Winter, A.; Spaleck, W.; Rohrmann, J. *Angew. Chem., Int. Ed. Engl.* **1989**, *28*, 1511−1512. (b) Herfert, N.; Fink, G. *Makromol. Chem., Rapid Commun.* **1993**, *14*, 91−96.

(16) Manriquez, J. M.; McAlister, D. R.; Sanner, R. D.; Bercaw, J. E. *J. Am. Chem. Soc.* **1978**, *100*, 2716−2724.

(17) Chien, J. C. W.; Tsai, W. M.; Rausch, M. D. *J. Am. Chem. Soc.* **1991**, *113*, 8570−8571.

warm to room temperature and stirred for 4 h. Subsequent removal of the solvent under vacuum afforded an orange powder. The powder was dissolved in CH_2Cl_2 (20 mL) and centrifuged to remove precipitated LiCl. The clear CH_2Cl_2 solution was decanted, then concentrated to about 10 mL, and pentane (30 mL) was transferred in under vacuum, layering it on top of the CH_2Cl_2 solution. Diffusion at room temperature overnight gave red crystalline $Ph_3C^+Nb(OC_6F_5)_6^-$ (1.97 g) in 95% yield. ^{1}H NMR (CD_2Cl_2, 23 °C): δ 8.28 (tr tr, 1 H, *m*-C_6H_5, J_{H-H} = 7.5/1.3 Hz), 7.89 (tr m, 2 H, *p*-C_6H_5, J_{H-H} = 8.0 Hz), 7.67 (d m, 2 H, *o*-C_6H_5, J_{H-H} = 8.5 Hz). ^{19}F NMR (CD_2Cl_2, 23 °C): δ −158.90 (d, 2 F, *o*-F, J_{F-F} = 17.2 Hz), −165.99 (tr, 2 F, *p*-F, J_{F-F} = 20.6 Hz), −169.56 (tr, 1 F, *m*-F, J_{F-F} = 22.0 Hz). Anal. Calcd for $C_{55}H_{15}O_6F_{30}Nb$: C, 46.05; H, 1.05; F, 39.73. Found: C, 45.69; H, 1.16; F, 40.13.

Synthesis of $Li(OEt_2)_3^+\{[Ta(OC_6F_5)_4(\mu_2\text{-}OC_6F_5)_2]_2Li\}\cdot C_7H_8$ (5b). Solid $TaCl_5$ (0.990 g, 2.76 mmol) and $LiOC_6F_5$ (3.14 g, 6 × 2.76 mmol) were added to a reaction flask in the glovebox. The flask was next transferred from the glovebox to the high-vacuum line. On the vacuum line, Et_2O (50 mL) was condensed in, and mixture stirred overnight at room temperature. After removing the Et_2O under vacuum, toluene (50 mL) was condensed in. The solution was next heated to 50 °C and filtered. Slow cooling of the filtrate to −20 °C gave yellow crystalline $[Li(OEt_2)_3]^+\{[Ta(OC_6F_5)_4(\mu_2\text{-}OC_6F_5)_2]_2Li\}\cdot C_7H_8$ (3.1 g) in 78% yield. ^{1}H NMR (C_6D_6, 23 °C): δ 3.04 (q, 4 H, $O(CH_2\text{-}CH_3)_2$ J_{H-H} = 7.1 Hz), 0.84 (tr, 6 H, $O(CH_2CH_3)_2$ J_{H-H} = 7.1 Hz). ^{19}F NMR (C_6D_6, 23 °C): δ −162.26 (br d, 2 F, *o*-F, J_{F-F} = 18.4 Hz), −163.73 (tr, 2 F, *p*-F, J_{F-F} = 21.2 Hz), −164.33 (tr, 1 F, *m*-F, J_{F-F} = 22.3 Hz). Anal. Calcd. for $C_{91}H_{38}O_{15}F_{60}Li_2Ta_2$: C, 37.86; H, 1.33; F, 39.48. Found: C, 37.95; H, 1.35; F, 38.98.

Synthesis of $Ph_3C^+Ta(OC_6F_5)_6^-$ (6b). $Li(OEt_2)_3^+\{[Ta(OC_6F_5)_4(\mu_2\text{-}OC_6F_5)_2]_2Li\}\cdot C_7H_8$ (0.689 g, 2.39 × 10^{-4} mol) and Ph_3CCl (0.137 g, 2 × 2.46 × 10^{-4} mol) were added to a reaction flask in the glovebox. The flask was next transferred from the glovebox to the high-vacuum line. On the vacuum line, pentane (50 mL) was condensed in. The mixture then was allowed to warm to room temperature and stirred for 4 h. Subsequent removal of the solvent under vacuum gave an orange powder. The powder was dissolved in CH_2Cl_2 (20 mL) and centrifuged to remove precipitated LiCl. After decanting, the clear CH_2Cl_2 solution was concentrated to about 10 mL and pentane (30 mL) was transferred in under vacuum, layering it on top of the CH_2Cl_2 solution. Diffusion at room temperature overnight gave red crystalline $Ph_3C^+Ta(OC_6F_5)_6^-$ (0.52 g) in 72% yield. ^{1}H NMR (CD_2Cl_2, 23 °C): δ 8.28 (tr tr, 1 H, *m*-C_6H_5, J_{H-H} = 7.5/1.3 Hz), 7.89 (tr m, 2 H, *p*-C_6H_5, J_{H-H} = 8.0 Hz), 7.67 (d m, 2 H, *o*-C_6H_5, J_{H-H} = 8.5 Hz). ^{19}F NMR (CD_2Cl_2, 23 °C): δ −159.40 (d, 2 F, *o*-F, J_{F-F} = 17.2 Hz), −166.02 (tr, 2 F, *p*-F, J_{F-F} = 21.2 Hz), −170.01 (tr, 1 F, *m*-F, J_{F-F} = 21.7 Hz). Anal. Calcd for $C_{55}H_{15}O_6F_{30}Ta$: C, 43.39; H, 0.99; F, 37.43. Found: C, 42.59; H, 1.02; F, 37.72.

Trapping of a Metallocenium Intermediate. To investigate the possible intermediacy of a cationic metallocene/anion complex in the activation process, $(C_5Me_5)_2ZrMe_2$ (5.0 mg, 1.28 × 10^{-2} mmol) and $Ph_3C^+Nb(OC_6F_5)_6^-$ (18.3 mg, 1.28 × 10^{-2} mmol) were weighed into a J. Young NMR tube in the glovebox. The tube was brought out of the box and interfaced to a high-vacuum line, and tetrahydrofuran-d_8 was condensed in at −78 °C. The tube was warmed to room temperature, and NMR spectra were immediately recorded. ^{1}H and ^{19}F NMR data (THF-d_8, 23 °C): δ 2.01 (s, 30 H, C_5Me_5), 0.40 (s, 3 H, Zr-*Me*). ^{19}F NMR (THF-d_8, 23 °C): δ −157.26 (d, 2 F, *o*-F, J_{F-F} = 18.1 Hz), −165.38 (tr, 2 F, *p*-F, J_{F-F} = 20.6 Hz), −169.14 (tr, 1 F, *m*-F, J_{F-F} = 22.9 Hz). The ^{19}F NMR data reveal that the $Nb(OC_6F_5)_6^-$ anion is intact and that no $OC_6F_5^-$ rings have been transferred to the cationic metallocene. The ^{1}H NMR shows an activated metallocene with characteristic downfield shifts for all protons. The ^{1}H data are also consistent with the published ^{1}H NMR data reported for $(C_5Me_5)_2ZrMe(THF)^+$-$B(C_6F_5)_4^-$ in C_6D_5Br: δ 1.55 (s, 30 H, C_5Me_5), 0.06 (s, 3 H, Zr-*Me*).[18]

In Situ Generation of Metallocene Pentafluorophenoxide Complexes. The reagent C_6F_5OH (35 mg) was charged into a 5.0 mL volumetric flask, and C_6D_6 was added until the total volume reached 5.0 mL. Next, 6.2 mg of *rac*-$Me_2Si(Ind)_2ZrMe_2$ was charged into a serum-capped NMR tube, and 0.7 mL of C_6D_6 was added. ^{1}H and ^{19}F NMR spectra of the NMR tube were then recorded after the successive addition of 0.0, 0.1, 0.2, 0.3, 0.4, 0.5, 0.6, 0.7, 0.8, and 1.2 mL aliquots of the C_6F_5OH/C_6D_6 solution (0.1 mL is approximately equal to 0.25 molar equiv of C_6F_5OH:Zr complex).

The initial aliquot of C_6F_5OH forms structures assignable to both *rac*-$Me_2Si(Ind)_2Zr(OC_6F_5)Me$ [^{19}F NMR (C_6D_6, 23 °C): δ −163.47 (dd, 2 F, *o*-F, $^3J_{FF}$ = 19.2 Hz, $^4J_{FF}$ = 7.6 Hz), −167.42 (dd, 2 F, *m*-F, $^3J_{FF}$ = 22.9 Hz, $^3J_{FF}$ = 19.2 Hz), −173.85 (tt, 1 F, *p*-F, $^3J_{FF}$ = 22.9 Hz, $^4J_{FF}$ = 7.1 Hz)] and *rac*-$Me_2Si(Ind)_2Zr(OC_6F_5)_2$ [^{19}F NMR (C_6D_6, 23 °C): δ −163.66 (dd, 2 F, *o*-F, $^3J_{FF}$ = 16.8 Hz, $^4J_{FF}$ = 3.8 Hz), −167.04 (dd, 2 F, *m*-F, $^3J_{FF}$ = 22.9 Hz, $^3J_{FF}$ = 19.2 Hz), −173.05 (tt, 1 F, *p*-F, $^3J_{FF}$ = 22.4 Hz, $^4J_{FF}$ = 6.6 Hz)] in a 6:1 ratio, respectively. The second through fourth aliquots of C_6F_5OH solution continue to form the same products in similar ratios. Aliquots 5 and 6 show increased amounts of *rac*-$Me_2Si(Ind)_2Zr(OC_6F_5)_2$ relative to *rac*-$Me_2Si(Ind)_2Zr(OC_6F_5)Me$. The seventh aliquot shows >95% of the *rac*-$Me_2Si(Ind)_2Zr(OC_6F_5)_2$ product. Further aliquots show free C_6F_5OH [^{19}F NMR (C_6D_6, 23 °C): δ −163.95 (dd, 2 F, *o*-F, $^3J_{FF}$ = 18.6 Hz, $^4J_{FF}$ = 5.1 Hz), −165.00 (dd, 2 F, *m*-F, $^3J_{FF}$ = 22.2 Hz, $^3J_{FF}$ = 18.2 Hz), −179.56 (tt, 1 F, *p*-F, $^3J_{FF}$ = 22.9 Hz, $^4J_{FF}$ = 5.6 Hz)] in solution.

Synthesis of Nonafluorobiphenyl-2-ol (PBOH). The reagent 2-bromononafluorobiphenyl (21.0 g, 0.053 mol) was charged into a reaction flask interfaced to a Schlenk line, and 150 mL each of freshly distilled Et_2O and pentane were added via syringe. The solution was next cooled to −78 °C and *n*-butyllithium (33.2 mL, 1.6 M in hexanes, 0.053 mol) added. The reaction mixture was stirred for 3 h at −78 °C, boron trichloride (17.7 mL, 1.0 M in hexanes, 0.017 mol) was added, and the reaction mixture was stirred overnight. Solvent was then removed in vacuo, 100 mL of 50% H_2O_2 (**Caution**: 50% H_2O_2 is dangerous; proper handling is required) containing 3.0 g of KOH was added at 0 °C, and the reaction mixture was stirred for 12 h. The product was then extracted with CH_2Cl_2, solvent was removed, and distillation at 120 °C/10^{-6} Torr gave 9.0 g of PBOH in 51% yield as a colorless oil. ^{19}F NMR (C_6D_6, 25 °C): δ −139.07 (d, 2 F, F-2′/6′), $^3J_{FF}$ = 22.6 Hz), − 139.74 (d, 1 F, F-3, $^3J_{FF}$ = 23.7 Hz), −151.95 (t, 1 F, F-4′, $^3J_{FF}$ = 21.4 Hz), −153.36 (t, 1 F, F-4, $^3J_{FF}$ = 21.7 Hz), −161.94 (dd, 2 F, F-3′/5′, $^3J_{FF}$ = 22.8 Hz, $^4J_{FF}$ = 7.1 Hz), −162.97 (dd, 1 F, F-6, $^3J_{FF}$ = 21.2 Hz, $^4J_{FF}$ = 8.7 Hz), −167.23 (t, 1 F, F-5, $^3J_{FF}$ = 22.7 Hz). ^{1}H NMR (C_6D_6, 25 °C): δ 4.27 (s, 1 H). Anal. Calcd. for $C_{12}F_9OH$: C, 43.40; H, 0.30. Found: C, 43.88; H, 0.77.

Synthesis of $Y(PBO)_3(PBOH)$ (9a). Solid $Y[CH(SiMe_3)_2]_3$ (0.254 g, 4.48 × 10^{-4} mol) was charged into a reaction flask in the glovebox. The flask was then transferred to the high-vacuum line. Under vacuum, hexanes (25 mL) were condensed in. At −78 °C, a pentane solution of PBOH (0.595 g, 4 × 4.48 × 10^{-4} mol, 10 mL) was then added slowly via syringe. The mixture was stirred for 30 min at −78 °C, then slowly warmed to room temperature and stirred for an additional 2 h. Filtration, washing with pentane, and drying under vacuum gave an off-white powder of $Y(PBO)_3(PBOH)$ in 80% yield. ^{19}F NMR (C_6D_6, 25 °C): δ −136.0 (br, s, 4 F), −140.0 (br, s, 8 F), −151.3 (br, s, 4 F), −154.9 (br, s, 4 F), −161.3 (br, s, 8 F), −162.1 (br, s, 4 F), −167.2 (br, s, 4 F). ^{1}H NMR (C_6D_6, 25 °C): δ 4.19 (s, H^+). Anal. Calcd for $C_{48}HO_4F_{36}Y$: C, 40.76; H, 0.07; F, 48.36. Found: C, 40.39; H, 0.54; F, 48.46.

Synthesis of $La(PBO)_3(PBOH)$ (9b). On the high-vacuum line, a pentane solution of $La[CH(SiMe_3)_2]_3$ (0.561 g, 9.09 ×

(18) Horton, A. D. *Organometallics* **1996**, *15*, 2675−2677.

10^{-4} mol) was charged into a reaction flask and cooled to −78 °C, and a pentane solution of PBOH (1.208 g, $4 \times 9.09 \times 10^{-4}$ mol, 25 mL) was added slowly via syringe. The mixture was immediately warmed to room temperature and stirred for an additional 2 h. Filtration, washing with pentane, and drying under vacuum gave an off-white powder of $La(PBO)_3(PBOH)$ in 56% yield. ^{19}F NMR (C_6D_6, 25 °C): δ −136.7 (br, s, 1 F), −140.2 (br, s, 2 F), −151.2 (br, s, 1 F), −155.5 (br, s, 1 F), −160.7 (br, s, 2 F), −162.3 (br, s, 1 F), −168.6 (br, s, 1 F). ^1H NMR (C_6D_6, 25 °C): δ 4.20 (s, H^+). Anal. Calcd for $C_{48}HO_4F_{36}La$: C, 39.37; H, 0.07; F, 46.71. Found: C, 39.03; H, 0.32; F, 45.47.

Reaction of Cp_2ZrMe_2 with $Y(PBO)_3(PBOH)$. In the glovebox, $Y(PBOH)(PBO)_3$ (30.1 mg, 2.12×10^{-2} mmol) and Cp_2ZrMe_2 (5.3 mg, 2.12×10^{-2} mmol) were charged in to a J. Young NMR tube, and toluene-d_8 (ca. 1 mL) was added. The solution immediately turned light yellow, and gas (CH_4) was evolved. The tube was then removed from the glovebox, and NMR spectra were recorded within ca. 5 min. The solution consisted of a complex mixture that appeared to contain Cp_2ZrMe^+, $[Cp_2ZrMe(\mu\text{-}Me)MeZrCp_2]^+$, and $Cp_2Zr(PBO)Me$ species. ^{19}F NMR (C_7D_8, 25 °C): δ −138.93 (d, 2 F, F-2′/6′), $^3J_{FF}$ = 21.4 Hz), − 141.55 (d of d, 1 F, F-3, $^3J_{FF}$ = 22.7, $^4J_{FF}$ = 3.2 Hz), −153.74 (t, 1 F, F-4′, $^3J_{FF}$ = 21.4 Hz), −155.08 (t, 1 F, F-4, $^3J_{FF}$ = 22.0 Hz), −162.57 (d of t, 2 F, F-3′/5′, $^3J_{FF}$ = 22.1 Hz, $^4J_{FF}$ = 7.1 Hz), −164.09 (d of t, 1 F, F-6, $^3J_{FF}$ = 13.6 Hz, $^4J_{FF}$ = 6.6 Hz), −171.07 (d of t, 1 F, F-5, $^3J_{FF}$ = 22.1 Hz, $^4J_{FF}$ = 4.6 Hz). Also present in the ^{19}F NMR are broad (e.g., 1.0 to 3.0 ppm) peaks centered around −139, −155, and −162. ^1H NMR (C_7D_8, 25 °C): δ −1.23 (s, $Cp_2ZrMe(\mu\text{-}CH_3)Zr(Me)Cp_2$), −0.16 (s, $Cp_2Zr(PBO)Me$), 0.03 (s, $Cp_2ZrMe(\mu\text{-}CH_3)Zr(Me)Cp_2$), 0.18 (s, CH_4) 0.49 (s, Cp_2ZrMe^+), 5.55 (s, $Cp_2Zr(PBO)Me$), 5.65, 5.68 (s, $Cp_2ZrMe(\mu\text{-}CH_3)Zr(Me)Cp_2$), 5.80 (s, Cp_2ZrMe^+).

Reaction of Cp_2ZrMe_2 with PBOH. To verify the existence of $Cp_2Zr(PBO)Me$ in the reaction mixture of Cp_2ZrMe_2 + $Y(PBOH)(PBO)_3$, an authentic sample of $Cp_2ZrMe(PBO)$ was generated. In the glovebox, Cp_2ZrMe_2 (5.0 mg, 1.99×10^{-2} mmol) and PBOH (6.6 mg, 1.99×10^{-2} mmol) were charged into a J. Young NMR tube, and toluene-d_8 was added. Unreacted Cp_2ZrMe_2, $Cp_2Zr(PBO)Me$, and $Cp_2Zr(PBO)_2$ can be seen in the NMR in roughly a 3:6:1 ratio. ^1H NMR: δ −0.21 (s, 6 H, $Cp_2Zr\mathit{Me}_2$), −0.20 (s, 3 H, $Cp_2Zr(PBO)\mathit{Me}$), 5.57 (s, 10 H, $\mathit{Cp}_2Zr(PBO)Me$), 5.61 (s, 10 H, $Cp_2Zr(PBO)_2$), 5.70 (s, 10 H, Cp_2ZrMe_2). ^{19}F NMR for $Cp_2Zr(PBO)Me$ (C_7D_8, 25 °C): δ −138.59 (d, 2 F, F-2′/6′), $^3J_{FF}$ = 22.8 Hz), −141.55 (d, 1 F, F-3, $^3J_{FF}$ = 23.1), −153.50 (t, 1 F, F-4′, $^3J_{FF}$ = 21.3 Hz), −154.84 (t, 1 F, F-4, $^3J_{FF}$ = 21.6 Hz), −162.37 (t, 2 F, F-3′/5′, $^3J_{FF}$ = 21.4 Hz), −163.88 (d, 1 F, F-6, $^3J_{FF}$ = 18.9 Hz), −170.90 (t, 1 F, F-5, $^3J_{FF}$ = 24.3 Hz). ^{19}F NMR for $Cp_2Zr(PBO)_2$ (C_7D_8, 25 °C): δ −138.35 (d, 4 F, F-2′/6′), $^3J_{FF}$ = 21.4 Hz), −140.05 (d, 2 F, F-3, $^3J_{FF}$ = 24.3), −153.04 (t, 2 F, F-4′, $^3J_{FF}$ = 21.2 Hz), −154.41 (t, 2 F, F-4, $^3J_{FF}$ = 21.3 Hz), −162.12 (peak partially under a $Cp_2Zr(PBO)Me$ peak) (t, 4 F, F-3′/5′, $^3J_{FF}$ = 21.7 Hz), −163.12 (d, 2 F, F-6, $^3J_{FF}$ = 21.2 Hz), −169.12 (t, 2 F, F-5, $^3J_{FF}$ = 20.0 Hz).

General Procedure for Single-Crystal Structural Characterization of Compounds 5a, 5b, 6a, 6b, and 7. Inside the glovebox, crystals were placed on a glass slide and covered with dry Infineum V8512 (formerly Paratone-N) oil. The crystals were then removed from the box, and a suitable crystal was chosen under a microscope using plane-polarized light. The crystal was mounted on a glass fiber and transferred to the cold stage of a Bruker SMART 1000 CCD area detector having a nitrogen cold-stream at 153(2) K. Twenty frames (usually 20 s exposures, 0.3° slices) were collected in three areas of reciprocal space to determine the orientation matrix. The parameters for data collection were determined by the peak intensities and widths from the 60 frames used to determine the orientation matrix. The faces of the crystal were then indexed, and data collection was started. After data collection, the frames were integrated, the initial crystal structure was solved by direct methods, the structure solution was expanded through successive least-squares cycles, absorption corrections were applied, and the final solution was determined. Further details of the structural refinements are given in Tables 2, 5, and 8 and in the Supporting Information.

Ethylene, Propylene Polymerization Experiments. This polymerization procedure is designed to minimize mass transfer (gas to solution; catalyst entrainment) and exotherm effects while at the same time maintaining strictly vacuum line-quality anaerobic/anhydrous conditions.[5k,l,n,6a] Polymerization activities of this magnitude measured by this procedure have previously been found to be in reasonable agreement with those measured in large-scale batch reactors.[5c] On the high vacuum line (10^{-6} Torr), ethylene and propylene polymerization reactions were carried out in 250 mL round-bottom three-neck Morton flasks equipped with large magnetic stirring bars and thermocouple probes. In a typical experiment (all experiments were carried out in triplicate), toluene (100 mL) was vacuum-transferred into the flask containing either $(C_5Me_5)_2ZrMe_2$ or $(C_5Me_4H)_2ZrMe_2$, and the reactor was saturated with 1.0 atm of ethylene or propylene (pressure control using an Hg bubbler) and equilibrated at the desired reaction temperature using an external water bath. A toluene solution (2 mL) containing 1.0 equiv of cocatalyst was then quickly injected into the rapidly stirred solution using a gastight syringe with a flattened needle for spraying small droplets of solution. The temperature of the toluene solution in polymerization experiments was monitored using a thermocouple (OMEGA Type K thermocouple with a Model HH21 microprocessor thermometer). After a measured time interval (short to minimize mass transport and exotherm effects), the polymerization was quenched by the addition of 20 mL of acidified (2% HCl) methanol. Another 100 mL of methanol was then added, and the polymer was collected by filtration, washed with methanol, and dried on the high-vacuum line overnight to a constant weight.

Ethylene and Propylene Copolymerization Experiments. Using the polymerization setup described above, a toluene solution (100 mL) of the catalyst was initially saturated with 1.0 atm pressure of propylene at 25 °C. The vessel was then reconfigured to admit 1.0 atm pressure of ethylene. After saturation with ethylene at −78 °C for 5 min, the vessel was warmed and equilibrated at 25 °C. A toluene solution (2 mL) containing 1.0 equiv of cocatalyst was then quickly injected into the rapidly stirred flask using a gastight syringe and the polymerization reaction subsequently quenched with 20 mL of acidic methanol after a measured time interval.

Alternative Parallel Polymerization Procedure. To increase the throughput of multiple polymerizations under identical conditions and to improve the precision of multiple polymerization runs, the following modified polymerization protocol was employed. In the glovebox, three polymerization reactors, 250 mL Morton style flasks equipped with type K thermocouples and large magnetic stirring bars, were filled with 100 mL of toluene (previously vacuum transferred from Na/K alloy on a high-vacuum line) via a 100.0 mL volumetric flask. The reactors were removed from the glovebox and then interfaced to the high-vacuum line and an Omega OM-3001 4 channel thermocouple data logger. The data logger is configured to record each channel every 0.6 s; channels 1−3 are the respective polymerization reactors, and channel 4 is the water bath. The three polymerization reactors were immersed in a large-capacity water bath to control the temperature. The reactors were degassed with successive vacuum cycles and back-filled with 1.0 atm of monomer. In the glovebox, the cocatalyst was weighed out and added to a 10.0 mL volumetric flask, which was then filled with ca. 5 mL of toluene. The flask was capped and shaken to completely dissolve the cocatalyst. The catalyst precursor was then weighed out and added to the volumetric flask, and toluene was added to bring the total

Scheme 1. Preparation of Complexes 5 and 6

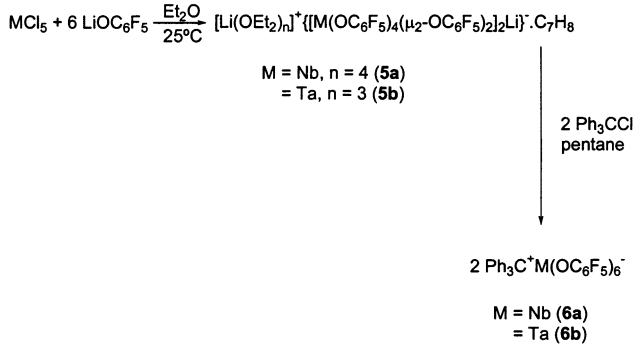

volume of the solution to 10.0 mL. The flask was next capped and shaken to ensure a homogeneous solution. Three aliquots of the catalyst (usually 2.0 mL) were withdrawn from the flask using 5.0 mL graduated, gastight syringes equipped with deflected-point needles. The syringes were removed from the glovebox with the needles inserted into silicone-capped, screw-top vials, and the contents were rapidly injected into the rapidly stirred polymerization reactors. After measured time intervals, the polymerizations were quenched with 20 mL of acidic (2% HCl) methanol. The polymer was precipitated with 100 mL of methanol, filtered, and dried to a constant weight under vacuum.

In cases where catalyst lifetime was limited and activation was known to be rapid, a modified procedure was employed. The cocatalyst and precatalyst were prepared in separate 10.0 mL toluene solutions, and aliquots of the cocatalyst were added to the reactors before they were removed from the glovebox. Then, aliquots of the precatalyst were loaded into syringes, and the remainder of the polymerization procedure was as previously described (vide supra). These procedures increase the precision of polymerization runs by ensuring the amount and concentration of catalysts are equal for each run. Simultaneous utilization of the same solvent batch, monomer stream, and water bath ensures polymerization conditions for each reactor are as close as possible to the other reactors.

Results and Discussion

Synthesis of Pentafluorophenoxide-Based Cocatalysts. The reaction of $LiAlH_4$ with HOC_6F_5 affords $Li^+Al(OC_6F_5)_4^-$,[19] and subsequent metathesis with Ph_3CCl yields the corresponding trityl tetrakis(pentafluorophenoxy)aluminate salt, $Ph_3C^+Al(OC_6F_5)_4^-$ (**4**; eq 1). Compound **4** is thermally stable at 25 °C in CD_2Cl_2 solution for days without noticeable decomposition and was characterized using standard analytical techniques (see Experimental Section for details).

$$LiAlH_4 + 4\ HOC_6F_5 \xrightarrow[-H_2]{\text{toluene, 85 °C}} Li^+Al(OC_6F_5)_4 \xrightarrow[-LiCl]{Ph_3CCl} Ph_3C^+Al(OC_6F_5)_4^- \quad (1)$$

The group 5 pentachlorides MCl_5 (M = Nb, Ta) readily undergo reaction with $LiOC_6F_5$ in Et_2O at 25 °C to afford crystalline $Li(OEt_2)_n^+\{[M(OC_6F_5)_4(\mu_2\text{-}OC_6F_5)_2]_2\text{-}Li\}\cdot C_7H_8$ salts (Scheme 1; M = Nb, $n = 4$ (**5a**); M = Ta, $n = 3$ (**5b**)), which were characterized using standard analytical methodology (see Experimental Section for details).[20] X-ray diffraction results (Figure 2) for **5b** (Tables 3, 4; bond angles and distances for **5a** are analogous) reveal a quasi-octahedral coordination geometry. Thus, *trans* O−Ta−O bond angles are 176.19(9)°, 172.94(8)°, and 171.62(7)°, and angles for *cis* O−Ta−O range from 88.07(8)° to 95.38(9)° excluding those involved in the square-planar Li^+ atom coordination, 79.95(7)°, for the oxygen atoms bridging the group 5 metal and lithium centers. The four nonbridging Ta−O distances range from 1.900(2) to 1.929(2) Å, while the distances for the two oxygen atoms bridging the metal and lithium centers are 2.031(2) and 2.033(2) Å. The group 5 centers are bridged by a slightly distorted square-planar Li^+ atom coordination (79.95(7)° for oxygen atoms bound to the same metal and 99.36(7)° for oxygen atoms bound to adjacent metal centers; Figure 2). The related structure of the pentakis(*p*-cresoxy)tantalum dimer,[21] $(CH_3OC_6H_4O)_4Ta(\mu\text{-}OC_6H_4OCH_3)_2\text{-}Ta(OC_6H_4OCH_3)_4$ (**I**), reveals a similar, although more distorted octahedral geometry around the Ta centers, with bond angles for *trans* O−Ta−O geometries = 176.9(4)°, 163.8(4)°, and 159.2(4)° and angles for *cis* O−Ta−O geometries ranging from 88.0(4)° to 105.2(4)°, excluding the 68.2(4)° for the μ-oxygen atoms bridging the Ta centers. The four nonbridging Ta−O distances range from 1.836(10) to 1.925(9) Å, with the distances for two oxygen atoms bridging the metal centers being 2.084(8) and 2.134(8) Å.

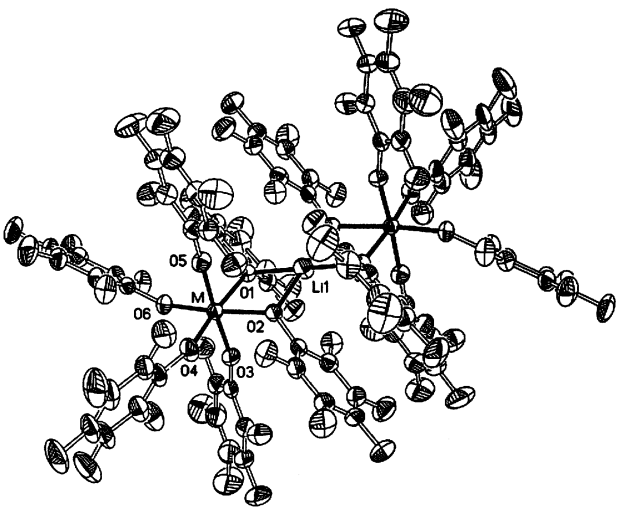

Figure 2. ORTEP plot (50% probabilities on thermal ellipsoids) of polynuclear perfluorophenoxide complexes **5**. M = Nb (**5b**).

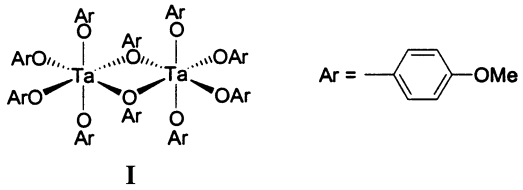

I

Compounds **5** are cleanly converted by metathesis with Ph_3CCl in pentane to the corresponding mononuclear, thermally stable $Ph_3C^+M(OC_6F_5)_6^-$ salts (M =

(19) The synthesis of related *fluoralkoxide* complex $Li^+[Al[OC(Ph)^-(CF_3)_2]_4]^-$ has been reported: Barbarich, T. J.; Handy, S. T.; Miller, S. M.; Anderson, O. P.; Grieco, P. A.; Strauss, S. H. *Organometallics* **1996**, *15*, 3776−3778.

(20) The synthesis of related *fluoroalkoxide* complexes $Ph_3C^+[Nb(OCH(CF_3)_2)_6]^-$ and $Li^+[Nb(OCH(CF_3)_2)_6]^-$ has been reported: Rockwell, J. J.; Kloster, G. M.; DuBay, W. J.; Grieco, P. A.; Shriver, D. F.; Strauss, S. H. *Inorg. Chim. Acta* **1997**, *263*, 195−200.

(21) Lewis, L. N.; Garbauskas, M. F. *Inorg. Chem.* **1985**, *24*, 363−366.

Table 1. Ethylene Polymerization Activities and Polymer Properties Using Pentafluorophenoxide-Based Cocatalysts[a]

entry	precursor	cocatalyst	μ mol of cat.	rxn time (s)	polymer yield (g)	activity g PE/atm.mol·h	M_n[b]	M_w/M_n	T_m[c] (°C)
1	$(C_5Me_5)_2ZrMe_2$	$Ph_3C^+Al(OC_6F_5)_4^-$ (**4**)	13.5	30	0.441	3.9×10^6	62 200	2.77	139.8
2	$(C_5Me_5)_2ZrMe_2$	$Ph_3C^+Nb(OC_6F_5)_6^-$ (**6a**)	12.7	30	0.498	6.0×10^6	45 800	3.32	138.7
3	$(C_5Me_5)_2ZrMe_2$	$Ph_3C^+Ta(OC_6F_5)_6^-$ (**6b**)	13.2	30	0.561	6.5×10^6	79 800	2.48	136.9
4	$(C_5Me_5)_2ZrMe_2$	$Ph_3C^+B(C_6F_5)_4^-$	17.6	30	0.636	4.3×10^6	88 200	2.15	137.9
5	$(C_5Me_4H)_2ZrMe_2$	$Ph_3C^+Al(OC_6F_5)_4^-$ (**4**)	18.1	30	0.471	3.1×10^6	127 000	1.91	137.2
6	$(C_5Me_4H)_2ZrMe_2$	$Ph_3C^+Nb(OC_6F_5)_6^-$ (**6a**)	17.3	30	0.549	4.1×10^6	106 000	3.30	136.8
7	$(C_5Me_4H)_2ZrMe_2$	$Ph_3C^+Ta(OC_6F_5)_6^-$ (**6b**)	17.5	30	0.739	5.0×10^6	62 500	4.03	136.5
8	$(C_5Me_4H)_2ZrMe_2$	$Ph_3C^+B(C_6F_5)_4^-$	17.3	30	0.729	5.1×10^6	33 200	7.60	135.9

[a] Carried out at 1.0 atm of ethylene pressure in 100 mL of toluene on a high-vacuum line at 25 °C. See Experimental Section and ref 5k for polymerization procedures. [b] GPC relative to polystyrene standards. [c] DSC trace from the second scan.

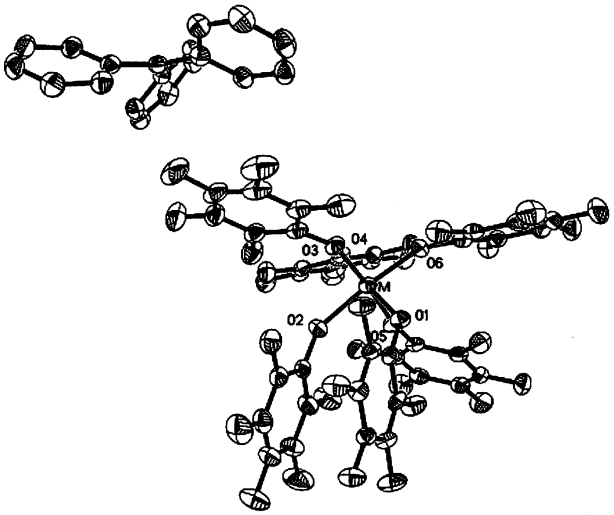

Figure 3. ORTEP plot (50% probabilities on thermal ellipsoids) of trityl perfluorophenoxymetalate cocatalysts **6**. M = Nb (**6a**).

Nb, (**6a**); M = Ta (**6b**)) in high yield (Scheme 1). These were characterized by standard techniques (see Experimental Section for details). Diffraction analysis for **6a** (Figure 3;Table 6) reveals six-coordinate metal centers with pronounced nonlinearity of the M−O−C_6F_5 linkages (Nb−O−C(aryl) ranges from 135.3(2)° to 170.6(2)°) and dispersion in Nb−O distances ranging from 1.913(2) to 2.009(2) Å. Metrical parameters for **6b** are similar (Table 7).Work by Parkin[22] and Rothwell[23] has shown that for early transition metal ions (Zr, Nb, Ta) there is little correlation between the M−O−C(aryl) bond angles and M−O bonding distances, and the structures presented here also exhibit little correlation between M−O bond distances and M−O−C(aryl) angles. The quasi-octahedral environment is maintained with *trans* O−Nb−O angles of 176.61(8)°, 173.62(8)°, and 170.56(8)° and *cis* O−Nb−O angles that range from 83.29(8)° to 94.59(8)°. A closely related structural analogue of **6**, the anion hexakis(3,5-dimethylphenoxy)-niobium, $Nb(OC_8H_9)_6^-$ (**II**),[24] has a less distorted octahedral geometry around the Nb center (*trans* O−Nb−O angles of 178.5(6)°, 177.6(6)°, and 176.9(6)° and *cis* O−Nb−O angles that range from 86.8(6)° to 92.5(6)°) with similar Nb−O bonding distances of 1.95(1)−1.98(1) Å. In contrast to **6a**, the Nb−O−C(aryl) angles of **II** also exhibit a much narrower dispersion in magnitude (142.6(1)−152.7(1)°).

Table 2. Summary of the Crystal Structure Data for Perfluorophenoxide Complexes 5

	5a	**5b**
formula	$C_{98}H_{48}F_{60}Li_2Nb_2O_{15}$	$C_{98}H_{48}F_{60}Li_2O_{15}Ta_2$
fw	2805.06	2981.14
cryst color, habit	yellow, needle	yellow, needle
cryst dimens, mm		
cryst syst	triclinic	triclinic
a, Å	14.5656(18)	14.5435(11)
b, Å	15.0032(18)	15.0132(11)
c, Å	15.4214(19)	15.4426(11)
α, deg	61.447(2)	61.270(1)
β, deg	63.499(2)	63.729(1)
γ, deg	88.445(2)	88.506(1)
volume, Å^3	2573.8(5)	2575.5(3)
space group	$P\bar{1}$ (#2)	$P\bar{1}$ (#2)
Z	2	2
D(calc), g/cm^3	1.810	1.922
μ, mm^{-1}	0.396	2.296
2θ range, deg	1.59 to 28.41	1.59 to 28.33
intensities (unique, R_i)	16 513 (11 486, 0.0322)	16 573 (11 437, 0.0138)
abs corr	SADABS	SADABS
no. data/restraints/ params	11 486/0/868	11 437/0/868
goodness-of-fit on F^2	0.979	1.050
final *R* indices [$I>2\sigma$]		
R	0.0615	0.0259
R_w^2	0.1597	0.0669
largest diff peak, hole, e$^-$/Å^3	1.451, −0.639	1.819, −1.004

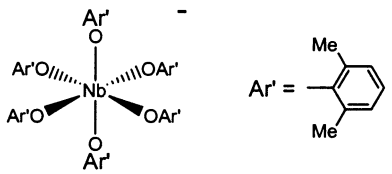

II

Reactivity of Representative Group 4 Metallocenes with Cocatalysts 6. The reactivity and cocatalytic characteristics of the trityl hexakis(pentafluorophenoxides) **6** were investigated with respect to a series of metallocene dimethyls to determine their suitability as activators in single-site olefin polymerization. At room temperature, facile $C_6F_5O^-$ transfer from Nb/Ta to Zr/Ti is observed for coordinatively more open group 4 complexes such as $(C_5H_5)_2ZrMe_2$, which reacts readily

(22) Howard, W. A.; Trnka, T. M.; Parkin, G. *Inorg. Chem.* **1995**, *34*, 5900−5909.

(23) (a) Steffey, B. D.; Fanwick, P. E.; Rothwell, I. P. *Polyhedron* **1990**, *9*, 963−968. (b) Coffindaffer, T. W.; Steffy, B. D.; Rothwell, I. P.; Folting, K.; Huffman, J. C. Streib, W. E. *J. Am. Chem. Soc.* **1989**, *111*, 4742−4749.

(24) Coffindaffer, T. W.; Steffy, B. D.; Rothwell, I. P.; Folting, K.; Huffman, J. C.; Streib, W. E. *J. Am. Chem. Soc.* **1989**, *111*, 4742−4749.

Table 3. Selected Bond Lengths (Å) and Bond Angles (deg) for $[Li(OEt_2)_4]^+\{[Nb(OC_6F_5)_4(\mu_2\text{-}OC_6F_5)_2]_2Li\}\cdot C_7H_8$ (5a)[a]

Nb(1)−O(1)	2.029(3)	Nb(1)−O(2)	2.029(3)
Nb(1)−O(3)	1.899(3)	Nb(1)−O(4)	1.895(3)
Nb(1)−O(5)	1.897(3)	Nb(1)−O(6)	1.935(3)
Nb(1)−Li(1)	3.1123(5)	O(1)−C(1)	1.351(4)
O(2)−C(7)	1.353(5)	O(3)−C(13)	1.332(5)
O(4)−C(19)	1.334(5)	O(5)−C(25)	1.329(5)
O(6)−C(31)	1.337(5)	O(1)−Li(1)	2.030(2)
O(2)−Li(1)	2.045(3)		
O(1)−Nb(1)−O(2)	80.03(10)	O(1)−Nb(1)−O(3)	88.64(13)
O(1)−Nb(1)−O(4)	173.90(11)	O(1)−Nb(1)−O(5)	88.37(12)
O(1)−Nb(1)−O(6)	91.31(11)	O(2)−Nb(1)−O(3)	90.03(12)
O(2)−Nb(1)−O(4)	93.88(12)	O(2)−Nb(1)−O(5)	88.07(12)
O(2)−Nb(1)−O(6)	171.34(11)	O(3)−Nb(1)−O(4)	91.01(15)
O(3)−Nb(1)−O(5)	176.70(13)	O(3)−Nb(1)−O(6)	89.67(12)
O(4)−Nb(1)−O(5)	91.81(14)	O(4)−Nb(1)−O(6)	94.78(12)
O(5)−Nb(1)−O(6)	91.80(12)	C(1)−O(1)−Nb(1)	135.4(2)
C(7)−O(2)−Nb(1)	129.3(2)	C(13)−O(3)−Nb(1)	165.3(3)
C(19)−O(4)−Nb(1)	161.0(3)	C(25)−O(5)−Nb(1)	172.5(3)
C(31)−O(6)−Nb(1)	149.6(3)	Nb(1)−O(1)−Li(1)	100.11(10)
Nb(1)−O(2)−Li(1)	99.61(10)	O(1)−Li(1)−O(2)#	100.38(10)
O(1)−Li(1)−O(2)	79.62(10)		

[a] Symmetry transformations used to generate equivalent atoms: # $-x+1, -y-1, -z-1$.

Table 4. Selected Bond Lengths (Å) and Bond Angles (deg) for $[Li(OEt_2)_3]^+\{[Ta(OC_6F_5)_4(\mu_2\text{-}OC_6F_5)_2]_2Li\}\cdot C_7H_8$ (5b)[a]

Ta(1)−O(1)	2.0331(17)	Ta(1)−O(2)	2.0308(18)
Ta(1)−O(3)	1.906(2)	Ta(1)−O(4)	1.900(2)
Ta(1)−O(5)	1.9042(19)	Ta(1)−O(6)	1.9292(18)
Ta(1)−Li(1)	3.1157(2)	O(1)−C(1)	1.353(3)
O(2)−C(7)	1.350(3)	O(3)−C(13)	1.332(4)
O(4)−C(19)	1.334(3)	O(5)−C(25)	1.329(3)
O(6)−C(31)	1.335(3)	O(1)−Li(1)	2.0203(17)
O(2)−Li(1)	2.0557(17)		
O(1)−Ta(1)−O(2)	79.95(7)	O(1)−Ta(1)−O(3)	88.52(9)
O(1)−Ta(1)−O(4)	172.94(8)	O(1)−Ta(1)−O(5)	88.07(8)
O(1)−Ta(1)−O(6)	91.67(8)	O(2)−Ta(1)−O(3)	89.61(9)
O(2)−Ta(1)−O(4)	93.00(8)	O(2)−Ta(1)−O(5)	88.12(8)
O(2)−Ta(1)−O(6)	171.62(7)	O(3)−Ta(1)−O(4)	91.22(11)
O(3)−Ta(1)−O(5)	176.19(9)	O(3)−Ta(1)−O(6)	90.02(9)
O(4)−Ta(1)−O(5)	91.96(10)	O(4)−Ta(1)−O(6)	95.38(9)
O(5)−Ta(1)−O(6)	91.78(8)	C(1)−O(1)−Ta(1)	134.46(16)
C(7)−O(2)−Ta(1)	129.42(16)	C(13)−O(3)−Ta(1)	163.7(2)
C(19)−O(4)−Ta(1)	159.8(2)	C(25)−O(5)−Ta(1)	171.97(19)
C(31)−O(6)−Ta(1)	149.38(17)	Ta(1)−O(1)−Li(1)	100.46(7)
Ta(1)−O(2)−Li(1)	99.36(7)	O(1)−Li(1)−O(2)#	100.34(7)
O(1)−Li(1)−O(2)	79.66(7)		

[a] Symmetry transformations used to generate equivalent atoms: # $-x+1, -y-1, -z-1$.

to form, as assessed by $^1H/^{19}F$ NMR spectral comparison with authentic samples, $(C_5H_5)_2Zr(OC_6F_5)_2$, Ph_3CCH_3, and presumably $MeNb(OC_6F_5)_4$, as well as unidentified minor byproducts. Authentic samples of perfluoroaryloxide transfer products were synthesized by titration of a dilute C_6F_5OH solution in toluene-d_8 into a serum-capped NMR tube containing a solution of metallocene in toluene-d_8 (see Experimental Section for details).

NMR-scale reaction of cocatalyst **6a** with 1.0 equiv of *rac*-$Me_2Si(Ind)_2ZrMe_2$ proceeds in a similar fashion with formation of *rac*-$Me_2Si(Ind)_2Zr(OC_6F_5)Me$. In contrast, the behavior toward sterically encumbered metallocenes, e.g., $(C_5Me_4H)_2ZrMe_2$ and $(C_5Me_5)_2ZrMe_2$, is significantly different. Thus, reaction of **6a** with 1.0 equiv of each of these metallocenes in toluene-d_8 initially results in red oily products, typical of more ionic (more loosely ion-paired) species,[6a] as well as $(C_5Me_4H)_2Zr(OC_6F_5)Me$ or $(C_5Me_5)_2Zr(OC_6F_5)Me$, respectively. These latter assignments were confirmed by NMR spectral comparison with authentic samples generated by in situ C_6F_5OH titration with neutral dimethyl complexes. On standing at −20 °C in an NMR tube, the red oily material slowly converts to crystals of the metallocenium ion pair $(C_5Me_5)_2ZrOC_6F_5{}^+Nb(OC_6F_5)_6^-$ (**7**; Scheme 2), which were isolated in small quantities and characterized by X-ray diffraction.

The molecular structure of complex **7** (Figure 4; Table 9) features a $(C_5Me_5)_2ZrR^+$ fragment with normal bent metallocene metrical parameters,[5n] Cp(cent)−Zr−Cp(cent) angle of 137.8(13)°, Cp(cent)−Zr distances of 2.205(4) and 2.213(4) Å, and an average C(Cp)−Zr distance of 2.517(4) Å. The related structures $(C_5Me_5)_2ZrMe(THT)^+B(C_6H_5)_4^-$ [25] (THT = tetrahydrothiophene) and $(C_5Me_5)_2ZrMe^+MeB(C_6F_5)_3^-$ [5o] display Cp(cent)−Zr−Cp(cent) angles of 138.2(3)° and 136.6(5)° with average C(Cp)−Zr distances of 2.54(1) and 2.537(7) Å,

Table 5. Summary of the Crystal Structure Data for Perfluorophenoxide Complexes 6

	6a	6b
formula	$C_{55}H_{15}O_6F_{30}Nb$	$C_{55}H_{15}O_6F_{30}Ta$
fw	1434.58	1522.62
cryst color, habit	orange, cut needle	orange, needle
cryst dimens (mm)	0.25 × 0.15 × 0.10	0.53 × 0.10 × 0.09
cryst syst	monoclinic	monoclinic
a, Å	14.2798(6)	14.2781(10)
b, Å	14.3771(6)	14.4033(10)
c, Å	25.0458(11)	25.028(2)
α, deg	90.00	90.00
β, deg	96.9330(1)	96.9200(13)
γ, deg	90.00	90.00
volume, Å^3	5104.4(3)	5109.6(5)
space group	$P2_1/n$ (#14)	$P2_1/n$ (#14)
Z	4	4
D(calc), g/cm^3	1.867	1.979
μ, mm^{-1}	0.400	2.312
2*θ* range, deg	to 56.6	to 56.7
intensities (unique, R_i)	38 570 (12 600, 0.030)	33 026 (12 545, 0.034)
abs corr	face-centered, SADABS	face-centered, SADABS
no. of data/restraints/params	6862/0/829	7452/0/829
goodness-of-fit on F^2	1.17	1.11
final *R* indices [$I>3\sigma$]		
R	0.030	0.029
R_w^2	0.048	0.050
largest diff peak, hole, e$^-$/Å^3	0.77, −0.51	2.29, −1.60

Table 6. Selected Bond Lengths (Å) and Bond Angles (deg) for $Ph_3C^+Nb(OC_6F_5)_6^-$ (6a)

Nb(1)−O(1)	2.009(2)	Nb(1)−O(2)	1.978(2)
Nb(1)−O(3)	1.929(2)	Nb(1)−O(4)	1.968(2)
Nb(1)−O(5)	1.935(2)	Nb(1)−O(6)	1.913(2)
O(1)−C(1)	1.322(3)	O(2)−C(7)	1.324(3)
O(3)−C(13)	1.329(3)	O(4)−C(19)	1.337(3)
O(5)−C(25)	1.328(3)	O(6)−C(31)	1.327(3)
O(1)−Nb(1)−O(2)	87.31(8)	O(1)−Nb(1)−O(3)	93.97(8)
O(1)−Nb(1)−O(4)	176.61(8)	O(1)−Nb(1)−O(5)	90.94(8)
O(1)−Nb(1)−O(6)	83.29(8)	O(2)−Nb(1)−O(3)	87.70(8)
O(2)−Nb(1)−O(4)	94.59(8)	O(2)−Nb(1)−O(5)	88.46(8)
O(2)−Nb(1)−O(6)	170.56(8)	O(3)−Nb(1)−O(4)	88.91(8)
O(3)−Nb(1)−O(5)	173.62(8)	O(3)−Nb(1)−O(6)	92.00(8)
O(4)−Nb(1)−O(5)	86.32(8)	O(4)−Nb(1)−O(6)	94.84(8)
O(5)−Nb(1)−O(6)	92.62(8)	Nb(1)−O(1)−C(1)	135.3(2)
Nb(1)−O(2)−C(7)	150.2(2)	Nb(1)−O(3)−C(13)	153.9(2)
Nb(1)−O(4)−C(19)	137.4(2)	Nb(1)−O(5)−C(25)	170.6(2)
Nb(1)−O(6)−C(31)	148.6(2)		

Scheme 2. Proposed Reactivity Pattern of $(C_5Me_5)_2ZrMe_2$ with Cocatalyst 6a

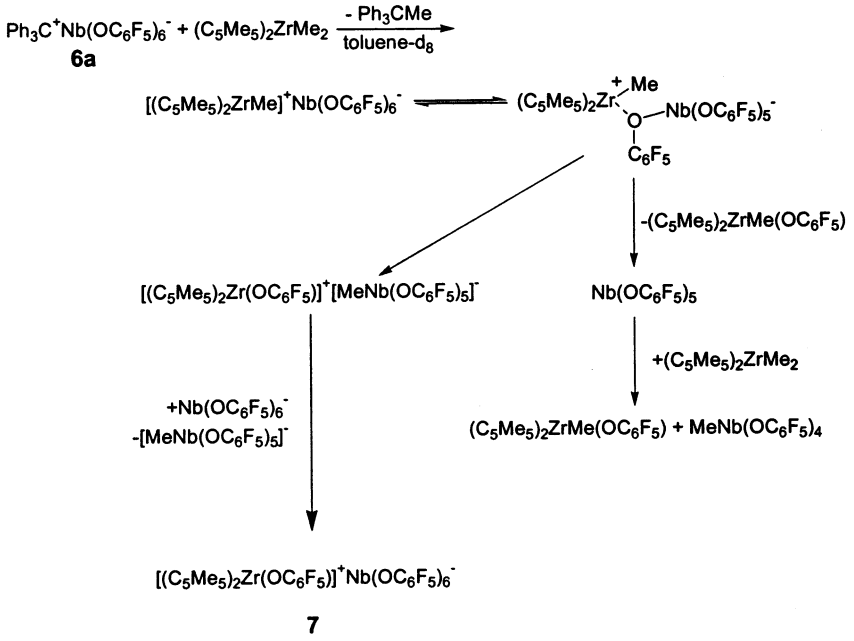

Table 7. Selected Bond Lengths (Å) and Bond Angles (deg) for $Ph_3C^+Ta(OC_6F_5)_6^-$ (6b)

Ta(1)−O(1)	2.000(3))	Ta(1)−O(2)	1.980(3))
Ta(1)−O(3)	1.926(3))	Ta(1)−O(4)	1.965(3))
Ta(1)−O(5)	1.931(3))	Ta(1)−O(6)	1.912(3))
O(1)−C(1)	1.327(5)	O(2)−C(7)	1.326(5)
O(3)−C(13)	1.344(5)	O(4)−C(19)	1.326(5)
O(5)−C(25)	1.335(4)	O(6)−C(31)	1.335(5)
O(1)−Ta(1)−O(2)	87.7(1)	O(1)−Ta(1)−O(3)	93.4(1)
O(1)−Ta(1)−O(4)	176.8(1)	O(1)−Ta(1)−O(5)	91.5(1)
O(1)−Ta(1)−O(6)	83.7(1)	O(2)−Ta(1)−O(3)	88.6(1)
O(2)−Ta(1)−O(4)	94.4(1)	O(2)−Ta(1)−O(5)	87.8(1)
O(2)−Ta(1)−O(6)	171.3(1)	O(3)−Ta(1)−O(4)	89.2(1)
O(3)−Ta(1)−O(5)	173.8(1)	O(3)−Ta(1)−O(6)	91.1(1)
O(4)−Ta(1)−O(5)	86.0(1)	O(4)−Ta(1)−O(6)	94.3(1)
O(5)−Ta(1)−O(6)	93.2(1)	Ta(1)−O(1)−C(1)	136.7(3)
Ta(1)−O(2)−C(7)	149.3(3)	Ta(1)−O(3)−C(13)	153.5(3)
Ta(1)−O(4)−C(19)	138.2(3)	Ta(1)−O(5)−C(25)	169.9(3)
Ta(1)−O(6)−C(31)	148.5(3)		

respectively. The Zr−O bond distance of 1.984(2) Å in structure **7** is indistinguishable from Zr−O bond distances of 1.989(3) Å found in $(C_5Me_5)Zr(OC_6H_5)_2$[26] and 1.991(2) Å found in $(C_5H_5)_2Zr(OC_6F_5)_2$.[27]

The geometry of the anionic $Nb(OC_6F_5)_6^-$ fragment in ion pair **7** is closer to octahedral than the analogous anion structures found in **6a** and **6b**, with *trans* O−Nb−O angles of 178.49(11)°, 176.44(11)°, and 174.76(11)° (vs 176.61(8)°, 173.62(8)°, and 170.56(8)° in structure **6a**) and *cis* O−Nb−O angles ranging from 86.84(11)° to 93.12(11)° (vs 83.29(8)−94.59(8)° in structure **6a**). Average Nb−O bond distances are equivalent for structures **6a** and **7** (**6a**, 1.955(2) Å, **7**, 1.946(3) Å), and both structures have similar dispersions in the Nb−O−C(aryl) angles (135.3(2)−170.6(2)° for **6a** and 136.2(2)−168.5(3)° for **7**).

Additionally, the molecular structure of complex **7** contains a relatively short $Zr^+\cdots$F−C(aryl) contact

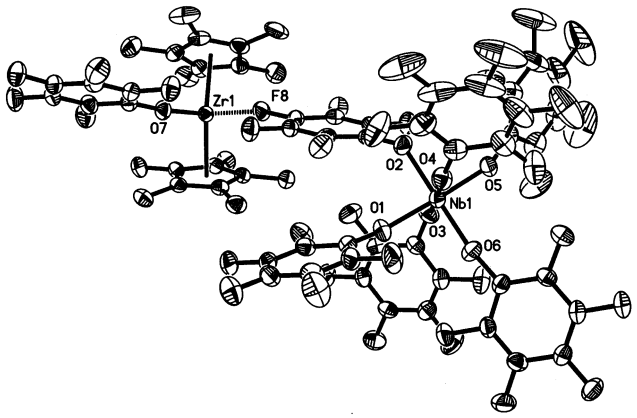

Figure 4. Solid-state structure of $[(C_5Me_5)_2Zr(OC_6F_5)]^+$-$Nb(OC_6F_5)_6^-$ (**7**). Selected bond distances (Å) and angles (deg): Zr1−Cent1 = 2.205(4); Zr1−Cent2 = 2.213(4); Zr1−F8 = 2.342(2); Zr1−O7 = 1.984(2); C10−F8 = 1.383(4); C−F(av) = 1.344(4); Nb−O(av) = 1.946(3); Cent1−Zr1−Cent2 = 1.378(13); F8−Zr1−O7 = 94.28(9); Zr1−O7−C37 = 168.0(3); Zr1−F8−C10 = 167.7(2); O1−Nb1−O5 = 176.44(11); O2−Nb1−O6 = 178.49(11); O3−Nb1−O4 = 174.76(11); smallest *cis* O−Nb1−O = 86.84(11); largest *cis* O−Nb1−O = 93.12(11).

(2.342(2) Å) and a correspondingly elongated F−C bond distance (1.383(4) vs 1.345(4) Å (av)). Such bonding patterns have been observed before in ion pairs composed of metallocenium cations and perfluoroarylate counteranions.[6c,28] This structural result argues for the intermediacy of $(C_5Me_5)_2ZrMe^+Nb(OC_6F_5)_6^-$ in the reaction of $(C_5Me_5)_2ZrMe_2$ and **6a**, as does observation of $(C_5Me_5)_2ZrMe(THF\text{-}d_8)^+Nb(OC_6F_5)_6^-$ (**8**) in in situ reaction of activator **6a** with $(C_5Me_5)_2ZrMe_2$ in THF-d_8, and the observed olefin polymerization activity of this reaction product (vide infra). The instability of $(C_5Me_5)_2$-

(25) Eshuis, J. J. W.; Tan, Y. Y.; Meetsma, A.; Teuben, J. H. *Organometallics* **1992**, *11*, 362−369.
(26) Howard, W. A.; Trnka, T. M.; Parkin, G. *Inorg. Chem.* **1995**, *34*, 5900−5909.
(27) Amor, J. I.; Burton, N. C.; Cuenca, T.; Gomez-Sal, P.; Royo, P. *J. Organomet. Chem.* **1995**, *485*, 153−160.
(28) (a) Sun, Y.; Spence, R. E. v. H.; Piers, W. E.; Parvez, M.; Yap, G. P. A. *J. Am. Chem. Soc.* **1997**, *119*, 5132−5143. (b) Ruwwe, J.; Erker, G.; Froehlich, R. *Angew. Chem., Int. Ed. Engl.* **1996**, *35*, 80−82. (c) Horton, A. D.; Orpen, A. G. *Organometallics* **1991**, *10*, 3910−3918. (d) Pasynkiewicz, S. *Polyhedron* **1990**, *9*, 429−453.

Table 8. Summary of the Crystal Structure Data for Complex 7

formula	$C_{72.50}H_{38}O_7F_{35}ZrNb$
fw	1870.16
cryst color, habit	yellow, shard
cryst dimens (mm)	0.3 × 0.3 × 0.2
cryst syst	triclinic
a, Å	12.6785(5)
b, Å	16.2379(7)
c, Å	17.6165(7)
α, deg	95.4110(10)
β, deg	105.0270(10)
γ, deg	90.4730(10)
volume, Å^3	3485.1(2)
space group	$P\bar{1}$(#2)
Z	2
D(calc), g/cm^3	1.782
μ, mm^{-1}	0.464
2*θ* range, deg	to 56.6
intensities (unique, R_i)	22 696 (15 655, 0.021)
abs corr	emprical and SADABS
no. of data/restraints/params	10 332/0/1054
goodness-of-fit on F^2	1.90
final *R* indices [$I>2\sigma$]	
R	0.039
R_w^2	0.077
largest diff peak, hole, e$^-$/Å^3	0.68, −0.66

Table 9. Selected Bond Lengths (Å) and Bond Angles (deg) for $[(C_5Me_5)_2Zr(OC_6F_5)]^+Nb(OC_6F_5)_6^-$ (7)

		$Nb(OC_6F_5)_6^-$	
Nb(1)−O(1)	1.957(3)	Nb(1)−O(2)	1.990(3)
Nb(1)−O(3)	1.972(3)	Nb(1)−O(4)	1.935(3)
Nb(1)−O(5)	1.903(3)	Nb(1)−O(6)	1.919(3)
O(1)−C(1)	1.324(4)	O(2)−C(7)	1.327(4)
O(3)−C(13)	1.336(4)	O(4)−C(19)	1.328(4)
O(5)−C(25)	1.324(4)	O(6)−C(31)	1.327(4)
O(1)−Nb(1)−O(2)	89.89(11)	O(1)−Nb(1)−O(3)	87.70(11)
O(1)−Nb(1)−O(4)	90.75(11)	O(1)−Nb(1)−O(5)	176.44(11)
O(1)−Nb(1)−O(6)	90.90(12)	O(2)−Nb(1)−O(3)	86.84(11)
O(2)−Nb(1)−O(4)	88.16(11)	O(2)−Nb(1)−O(5)	87.45(11)
O(2)−Nb(1)−O(6)	178.49(11)	O(3)−Nb(1)−O(4)	174.76(11)
O(3)−Nb(1)−O(5)	89.79(11)	O(3)−Nb(1)−O(6)	91.90(11)
O(4)−Nb(1)−O(5)	91.53(11)	O(4)−Nb(1)−O(6)	93.12(11)
O(5)−Nb(1)−O(6)	91.71(11)	Nb(1)−O(1)−C(1)	155.3(3)
Nb(1)−O(2)−C(7)	136.2(2)	Nb(1)−O(3)−C(13)	140.4(2)
Nb(1)−O(4)−C(19)	153.9(3)	Nb(1)−O(5)−C(25)	156.5(2)
Nb(1)−O(6)−C(31)	168.5(3)		
		$(C_5Me_5)_2Zr(OC_6F_5)^+$	
Zr(1)−Cent(1)	2.205(4)	Zr(1)−Cent(2)	2.213(4)
Zr(1)−F(8)	2.342(2)	Zr(1)−O(7)	1.984(2)
C(10)−F(8)	1.383(4)	C−F (av)	1.344(4)
O(7)−C(37)	1.332(4)		
Cent(1)−Zr(1)−Cent(2)	137.8(13)	F(8)−Zr(1)−O(7)	94.28(9)
Zr(1)−O(7)−C(37)	168.0(3)	Zr(1)−F(8)−C(10)	167.7(2)

$ZrMe^+Nb(OC_6F_5)_6^-$ may reflect, among other factors, the aforementioned deformability of the Nb−O−C_6F_5 linkages, which would facilitate Nb−O−C_6F_5 interaction with, and subsequent $C_6F_5O^-$ transfer to, the electrophilic zirconium center.

Perfluorophenoxymetalate-Based Single-Site Polymerization Catalysts. The above results imply that phenoxide transfer from cocatalyst **6** is facile for sterically more open metallocenium systems, explaining why such preactivated catalysts are inactive toward olefin polymerization. However, spectroscopic observation of ion pair **8** prompted studies of in situ $(C_5Me_5)_2ZrMe_2$ and $(C_5Me_4H)_2ZrMe_2$ activation in the presence of olefin (as is commonly performed with relatively unstable $B(C_6F_5)_4^-$-based catalysts).[6a] Under such conditions, reaction of **4** and **6** with $(C_5Me_5)_2ZrMe_2$ and $(C_5Me_4H)_2ZrMe_2$ at 25 °C affords efficient ethylene polymerization catalysts (Table 1) with activities and product polymer properties comparable to those of $Ph_3C^+B(C_6F_5)_4^-$-activated systems under identical polymerization conditions. One unusual feature of the present catalysts is that high ethylene polymerization activity is *not* paralleled by high propylene polymerization activity. To our knowledge, this is the first report of such a large anion-modulated metallocene reactivity pattern.[29] However, propylene incorporation in ethylene + propylene copolymerizations is observed. The ability of the present catalyst systems to differentiate between $CH_2{=}CH_2$ and $CH_2{=}CHCH_3$ at the activation step may be related to secondary interactions of the anion phenoxide ligands with the cationic metallocene centers.

Perfluorobiphenoxymetalate Polymerization Catalysts. Since the utility of the aforementioned pentafluorophenoxy-based cocatalysts is to some degree limited by phenoxide group transfer to less encumbered cationic metallocenes, new synthetic approaches were explored to improve catalyst stability. Substituting pentafluorophenoxide substituents with nonafluorobiphenoxide substituents adds considerable steric bulk about the cocatalyst core and more effectively screens the oxygen atoms from the cationic metallocene electrophile. Reaction of 2-bromononafluorobiphenyl with 1 equiv of *n*-butyllithium at −78 °C and subsequent reaction with 0.33 equiv of boron trichloride generates tris(2,2′,2″-nonfluorobiphenyl)borane.[5l] After solvent removal in vacuo, 50% hydrogen peroxide and KOH were added at 0 °C. Stirring overnight, workup, and purification by high-vacuum distillation at 120 °C leads to pure nonafluorobiphenyl-2-ol (PBOH) in 51% yield (eq 2).

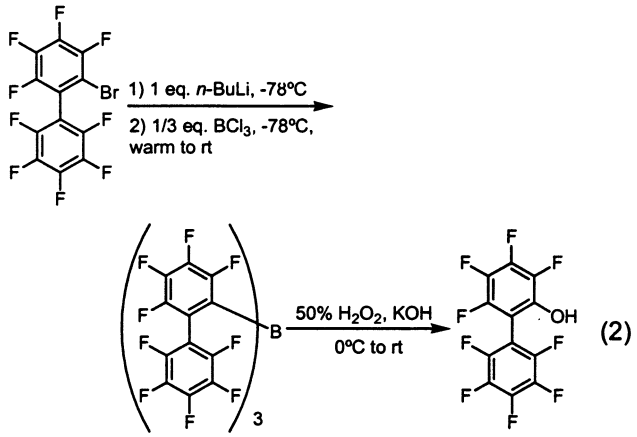

(2)

Initial attempts to synthesize the hexakis(nonafluorobiphenoxy)tantalum anions were unsuccessful, likely due to the severely crowded metal center that would be formed. Instead lithium pentakis(nonafluorobiphenoxy)tantalum chloride was isolated and characterized by X-ray diffraction.[30]

Next, a protonolytic route employing low coordination number oxophilic lanthanide hydrocarbyls was investigated. Reaction of $Ln(CH(SiMe_3)_2)_3$ (where Ln = Y,[11] La[12]) with 4.0 equiv of nonafluorobiphenyl-2-ol in pen-

(29) (a) Jia, L.; Yang, X.; Stern, C. L.; Marks, T. J. *Organometallics* **1997**, *16*, 842−857. (b) Yang, X.; Stern, C. L.; Marks, T. J. *J. Am. Chem. Soc.* **1994**, *116*, 10015−10031.

Table 10. Ethylene Polymerization Activities and Polymer Properties Using Ln(PBO)$_3$(PBOH)[a] Cocatalysts

catalyst precursor	cocatalyst	μmol cat.	polym time (s)	polymer (g)	M_n[b]	M_w/M_n	T_m[c] (°C)	activity[d,e]
$CGCZrMe_2$	Y(PBO)$_3$(PBOH)	16.5	1800	0.030			135	3.6×10^3
$CGCTiMe_2$	Y(PBO)$_3$(PBOH)	17.1	90	0.489	414 000	1.86	140	1.1×10^6
Cp_2ZrMe_2	Y(PBO)$_3$(PBOH)	16.3	30	0.720	307 100	2.12	139	5.3×10^6
$Me_2Si(Ind)_2ZrMe_2$	Y(PBO)$_3$(PBOH)	14.8	30	0.730	268 000	2.39	137	5.9×10^6
$(C_5Me_5)_2ZrMe_2$	Y(PBO)$_3$(PBOH)	14.6	30	0.603	182 800	2.56	141	5.0×10^6
$CGCTiMe_2$	La(PBO)$_3$(PBOH)	15.5	600	0.146	499 800	1.84	138	5.6×10^4
$(C_5Me_5)_2ZrMe_2$	La(PBO)$_3$(PBOH)	12.7	30	0.556	263 700	2.63	142	5.0×10^6

[a] Carried out at 1.0 atm of ethylene pressure in 100 mL of toluene on a high-vacuum line at 25 °C. [b] GPC relative to polystyrene standards. [c] DSC trace from second scan. [d] Activity in units of g polymer/mol catalyst·atm ethylene·h. [e] Activity is the average of three runs with approximately 10% reproducibility.

tane at room temperature results in the rapid and quantitative formation of Ln(PBO)$_3$(PBOH) complexes (eq 3). These products were characterized by standard analytical techniques (see Experimental Section for details). The exact location of the proton has not been determined, but it is presumably associated with an oxygen atom.[31] The ^{19}F NMR data are consistent with magnetically equivalent $C_{12}F_9^-$ groups in solution at room temperature.

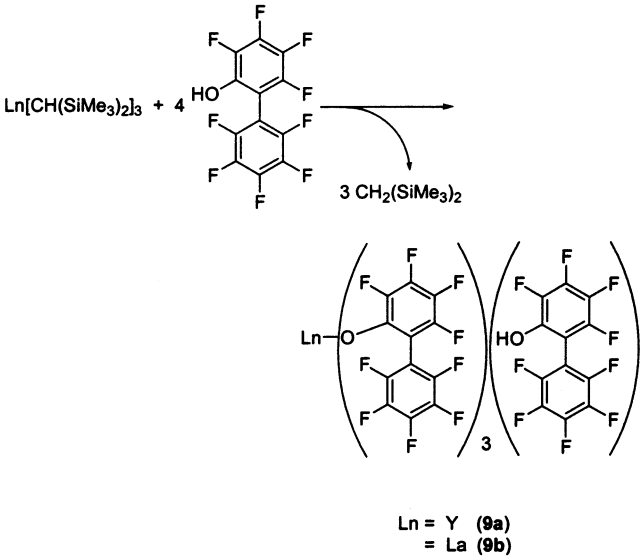

Reactivity of Perfluorobiphenoxide Complexes with Metallocene Dimethyls. The reactivity of cocatalysts **9a** and **9b** in the formation of single-site olefin polymerization catalysts was explored using a series of metallocene precatalysts. When **9a** or **9b** is mixed with metallocene dimethyls in hydrocarbon solvents, cation−anion pairs are formed immediately, as assessed by in situ NMR spectroscopy, immediate gas evolution, and immediate polymerization activity. In stark contrast to the pentafluorophenoxide-based cocatalysts discussed above, these cation−anion pairs are surprisingly stable over significant periods of time. Ion pairs of **9a** with either $(C_5Me_5)_2ZrMe_2$ or Cp_2ZrMe_2 are extremely active ethylene polymerization catalysts even after 4.0 h of standing at room temperature. In fact, samples used in unsuccessful crystallization experiments, which were carried out at room temperature for periods of up to 3 days, followed by standing in a −15 °C freezer for a week, still exhibited high activity for ethylene polymerization.

Further evidence for this increased ion pair stability can be seen in NMR data from the reaction of **9a** with either Cp_2ZrMe_2 or $(C_5Me_5)_2ZrMe_2$. Previous decomposition of perfluoroaryloxide-based cocatalysts (**6a**, **6b**) involved abstraction of an aryloxide ring from the cocatalyst by the cationic metallocenium electrophile. In the case of **9a**, the cationic metallocene interacts with the corresponding neutral metallocene to form the known μ-Me-bridged $Cp_2ZrMe(\mu\text{-}Me)MeZrCp_2^+$ and $(C_5Me_5)_2ZrMe(\mu\text{-}Me)MeZr(C_5Me_5)_2^+$ dimers derived from Cp_2ZrMe_2 and $(C_5Me_5)_2ZrMe_2$,[6c,32,5l] respectively. These dimers were identified by the characteristic upfield shift of the bridging $Zr(\mu\text{-}CH_3)Zr$ groups, δ −1.30 for the Cp_2Zr dimer and δ −2.43 for the $(C_5Me_5)_2Zr$ dimer, along with assignment of the remaining ^{1}H resonances. The tendency for metallocene μ-Me dimer formation is associated with counteranions having very weak coordinative tendencies.[6a]

Polymerization Characteristics of Perfluorobiphenoxide-Based Cocatalysts. When cocatalysts **9** are paired with a variety of metallocene precatalysts, rather active ethylene polymerization catalysts are formed (Table 10). Yttrium-based cocatalyst **9a** forms highly active (activity $>10^6$ g polymer/mol cat·atm monomer·h) polymerization systems when combined with a sterically varied array of organo-group 4 precatalysts. From sterically open $CGCTiMe_2$ to the sterically encumbered $(C_5Me_5)_2ZrMe_2$, **9a** forms highly active polymerization systems, in contrast to cocatalysts **4** and **6**, which are not compatible with sterically open metallocenes. In all likelihood, the severely encumbered perfluorobiphenyl rings block access to the oxygen atoms and stabilize what appear to be loosely bound ion pairs. The ability of **9a** and **9b** to effect the rapid polymeri-

(30) Reaction of 6 equiv of lithium nonafluorobiphenoxide with tantalum pentachloride in ether failed to form the desired hexakis(nonafluorobiphenoxy)tantalate anion. Rather, lithium pentakis(nonafluorobiphenoxy)tantalum chloride ($Li^+ClTa(PBO)_5^-$) was formed. Crystals suitable for single-crystal X-ray diffraction analysis were grown and reveal a crowded tantalum center surrounded by bulky perfluorobiphenoxy ligands. The crowded tantalum center is evidenced by the well-defined octahedral geometry (*trans* O−Ta−O or O−Ta−Cl angles of 177.4(2)°, 176.4(2)°, and 176.4(2)° with *cis* O−Ta−O or O−Ta−Cl angles falling in the narrow range of 87.0(1)−92.6(2)°), presumably to minimize interligand nonbonded contacts. In contrast, the structure of **6b**, $Ph_3C^+Ta(OC_6F_5)_6^-$, reveals a less sterically crowded Ta center, evident in the distorted octahedral environment discussed in the text (*trans* O−Ta−O angles of 176.8(1)°, 173.8(1)°, and 171.3(1)° with *cis* O−Ta−O ranging from 83.7(1)−94.4(1)°). Another factor indexing the steric crowding around the Ta center are the Ta−O−C(aryl) angles, which expand out to an average of 158.2(5)° for $Li^+ClTa(PBO)_5^-$ versus 149.4(3)° for **6b**.

(31) $(C_6F_5)_3B$·ROH complexes that have been used as cocatalysts, see: (a) Beringhelli, T.; Maggioni, D.; D'Alfonso, G. *Organometallics* **2001**, *20*, 4927−2938, and references therein. (b) Siedle, A. R.; Lamonna, W. M.; Newmark, R. A.; Stevens, J.; Richardson, D. E.; Ryan, M. *Makromol. Chem., Makromol. Symp.* **1993**, *66*, 215−224.

(32) (a) Bochmann, M.; Lancaster, S. J. *Angew. Chem., Int. Ed. Engl.* **1994**, *33*, 1634−1637. (b) Beck, S.; Prosenc, M. H.; Brintzinger, H. H.; Goretzki, R.; Herfert, N.; Fink, G. *J. Mol. Catal.* **1998**, *111*, 67−79.

zation of ethylene with open precatalysts such as $CGCTiMe_2$ and the extremely long lifetime of resultant cation−anion pairs demonstrate high stability with respect to perfluoroaryloxide ring transfer to the cationic metal center. Note also that the molecular weights of the **9**-derived polyethylenes are significantly higher than those from **4** and **6** (Table 1).

Conclusions

Highly efficient single-site cocatalysts containing neither group 13 elements nor metal/metalloid−carbon bonds have been synthesized and shown to form highly active ethylene polymerization catalysts when paired with sufficiently encumbered metallocenes. Although the new class of perfluorophenoxymetalate cocatalysts utilizing $C_6F_5O^-$ ligands is limited by facile perfluoroaryloxide ring transfer to cationic metallocenes with nonbulky ligands, the lifetime of the resultant active species is sufficient to demonstrate high polymerization activity.

Lanthanide-based cocatalysts (**9**) employing the perfluorobiphenoxide ligand form stable, highly active ethylene polymerization catalysts. Introduction of the nonafluorobiphenoxide ($2\text{-}C_{12}F_9O^-$) group has major consequences for stabilization of the perfluoroaryloxymetalate cocatalyst system. Not only are catalyst lifetimes longer, but even the most sterically open group 4 complexes, such as $CGCTiMe_2$ and Cp_2ZrMe_2, serve as precursors for active polymerization systems. Perfluoroaryloxide ring transfer is not completely inhibited by the increased steric bulk of **9**; however it is significantly retarded. As evidenced by the formation of cationic μ-methylmetallocene dimers, $Cp_2ZrMe(\mu\text{-}Me)MeZrCp_2^+$ and $(C_5Me_5)_2ZrMe(\mu\text{-}Me)MeZr(C_5Me_5)_2^+$, the metalate anions of **9** are weakly coordinating, much like $B(C_6F_5)_4^-$, and with similar ethylene polymerization cocatalytic characteristics.

Acknowledgment. This research was supported by the U.S. Department of Energy (DE-FG 02-86 ER13511). Y.S. thanks Dow Chemical Co. for a postdoctoral fellowship. We thank Dr. P. N. Nickias of Dow Chemical Co. for GPC analyses.

Supporting Information Available: Complete X-ray structural data, figures of polymerization apparatus, and a temperature profile of a typical parallel polymerization reaction. This material is available free of charge via the Internet at http://pubs.acs.org.

OM020087S